

Understanding Self-Supervised Learning via Gaussian Mixture Models

Parikshit Bansal[†]
 pbansal@utexas.edu

Ali Kavis[†]
 kavis@austin.utexas.edu

Sujay Sanghavi[†]
 sanghavi@mail.utexas.edu

[†]University of Texas at Austin

Abstract

Self-supervised learning attempts to learn representations from un-labeled data; it does so via a loss function that encourages the embedding of a point to be close to that of its augmentations. This simple idea performs remarkably well, yet it is not precisely theoretically understood why this is the case. In this paper we analyze self-supervised learning in a natural context: dimensionality reduction in Gaussian Mixture Models. Crucially, we define an augmentation of a data point as being another independent draw from the same underlying mixture component. We show that vanilla contrastive learning (specifically, the InfoNCE loss) is able to find the optimal lower-dimensional subspace even when the Gaussians are not isotropic – something that vanilla spectral techniques cannot do. We also prove a similar result for "non-contrastive" self-supervised learning (i.e., SimSiam loss). We further extend our analyses to multi-modal contrastive learning algorithms (e.g., CLIP). In this setting we show that contrastive learning learns the subset of fisher-optimal subspace, effectively filtering out all the noise from the learnt representations. Finally, we corroborate our theoretical finding through synthetic data experiments.

1 Introduction

Contrastive learning (CL) is now a gold-standard paradigm for learning representations with popular examples such as vision models like SimCLR Chen et al. [2020a] and MoCo Chen et al. [2020b], text models like Dense Passage Retrieval (DPR) Karpukhin et al. [2020], and vision-language models like CLIP Radford et al. [2021]. Once learned, these representations both demonstrate commendable zero-shot performance, and could easily be adapted to achieve SoTA performance on various tasks like classification Chen et al. [2020a] and retrieval Izacard et al. [2021].

Essentially, contrastive learning is a self-supervised strategy that aims to learn consistent representations given a set of unlabeled dataset. The core idea is to relate *similar* (positive) data samples to each other while contrasting *unrelated* (negative) points to dissociate them. To formalize, consider a pair of points $(\mathbf{x}, \hat{\mathbf{x}})$, where \mathbf{x} is some point from the dataset and $\hat{\mathbf{x}}$ is a "similar", positive example. CL methods learn representations so that the embedding of the point \mathbf{x} is *close* to that of its partner $\hat{\mathbf{x}}$, while being *far away* from the embedding of other points. Sometimes, these pairs are naturally present. For instance, in vision-language settings like CLIP, each training data comes as a pair of an image and the corresponding text caption. In other scenarios, they can be manually obtained via data augmentation that preserves the underlying semantics, e.g., we can define an image and its resized/cropped/rotated version as a pair.

It is fundamentally important to understand **why this simple idea of relating/contrasting pairs works so well**. In this paper, we aim to answer this question by a theoretical study of contrastive learning in a classic setting: dimensionality reduction in Gaussian Mixture Models (GMMs).

To motivate our study for contrastive learning, let us take a particular representation learning perspective. Essentially, representation learning aims at finding a (non-convex) mapping between the high-dimensional input space of data, e.g., natural images of 1 million pixels, and a lower dimensional output domain of their *representations*, e.g., 1024-dimensional feature vectors. Similarly, contrastive learning aims at discovering robust mappings between the data and the representations by exploiting additional information in the form of augmentations. In our framework of GMMs, we consider *linear* mappings/projections (for analytical tractability) and characterize the *optimality* (more on this in Section 3) of the mapping functions learned by contrastive methods by analyzing the associated projection subspaces. An integral components of our work is a key, novel notion of augmentations in the context of GMMs.

To highlight the success of contrastive methods in learning linear projectors, we conduct our study in comparison to standard spectral methods. i.e., based on singular value decomposition (SVD). We provide an example where spectral methods fall short of contrastive methods in finding anticipated projection subspaces (see Section 4.3). At this point, we would like to emphasize the main difference between contrastive methods and SVD-based methods; while contrastive learning methods leverage augmentations by design, the SVD-based methods cannot. Moreover, our endeavor is *not* to determine the better of the methods. In fact, we aim to show that *when augmentations are present*, contrastive learning can *provably* go beyond what would be possible otherwise. In that sense, our focus is on providing principled, theoretical insight into how contrastive learning works.

Within our GMM framework, a key, novel proposal of ours is formalizing the “notion of augmentations”, i.e. point-pairs. We assume that for every point \mathbf{x} drawn from the GMM, we are given an augmentation $\hat{\mathbf{x}}$, which is drawn from the same GMM based on a particular distribution (see Definition 5.1) that is biased towards the component that the original point \mathbf{x} belongs to. To keep the setting realistic, we are oblivious to which GMM component either of them come from.

Given pairs of points $(\mathbf{x}, \hat{\mathbf{x}})$ of the type described above, we analyze contrastive learning objectives in two categories; single and multi-modal GMMs. In the single modal setting, the points in a pair are drawn from the same GMM distribution. Under this setting, we analyze InfoNCE and SimSiam losses, which are suited to leverage the additional information provided by the augmentations unlike spectral methods. In the **multi-modal** context, the pair $(\mathbf{x}, \hat{\mathbf{x}})$ will be generated by *separate* GMMs. A fundamental example is the CLIP model, where images are associated with text descriptions such that the samples are pairs of the form $(\mathbf{x}_V, \mathbf{x}_T)$, where \mathbf{x}_V (images) and \mathbf{x}_T (texts) can have different dimensions. The objective now is to learn two different functions – two different linear projections – one for each modality, such that each modality is projected onto the same space. Contrastive learning in this context tries to make the final projection of \mathbf{x}_V close to that of pair \mathbf{x}_T , and far from random other $\hat{\mathbf{x}}_T$ ’s. Particularly, the framework for the multi-modal GMM has a major difference; we do not need augmentations. We provide further details in Section 6.

Contributions: Our objective is to theoretically understand the vital role augmentations in self-supervised representation learning; we do so in the context of GMMs. Precisely,

1. We formalize a mathematical notion of augmentation/point pairs – for both single and multi-modal GMMs, enabling us to concretely characterize contrastive learning methods in the context of GMMs.
2. We quantify a measure of optimality for the projections learned in the context of GMMs (see

Section 4). We show that InfoNCE can find optimal projections for GMMs with *general shared covariances*, whereas spectral methods cannot do so beyond *spherical* GMMs.

3. For the multi-modal GMM setting, we show that the CLIP contrastive loss learns linear projections that are a subset of the (Fisher-)optimal subspaces for each modality, i.e., filtering out all noise directions.

2 Related Work

Contrastive Learning and InfoNCE. Contrastive learning is widely used in current state-of-the-art representation learning methods like SimCLR Chen et al. [2020a], MoCo Chen et al. [2020b] etc. Prior theoretical work analysing contrastive learning argue that the contrastive objective leads to learning of good "general purpose" representations that can be used for better downstream performance and sample complexity. Arora et al. [2019] gives the first theoretical analyses of the contrastive loss, showing provable guarantees on downstream task with reduced sample complexity. HaoChen et al. [2021] relaxes the augmentation assumptions made in Arora et al. [2019] by showing that contrastive learning is equivalent to spectral clustering on some appropriately defined data graph. Saunshi et al. [2022], HaoChen and Ma [2022] extend this line of work by arguing for the inclusion of the inductive biases of the neural network architecture into the theoretical analyses.

Self-supervised Learning. Apart from contrastive methods, BYOL Grill et al. [2020], SwAV Caron et al. [2020], SimSiam Chen and He [2021] are also popular methods for self-supervised representation learning. These methods are also based on Siamese architecture used in contrastive methods, but notably don't rely on negatives to prevent a "collapsing" solution. Contrastive methods like SimCLR Chen et al. [2020a] and CLIP Radford et al. [2021] aim to learn representations so that embedding of a point is close to its partner in the pair while far away from embedding of a random other point. The non-contrastive self-supervised learning methods enforce just the former condition. These methods empirically work by breaking the symmetry between the Siamese towers Wang et al. [2022]. Prediction head, momentum encoder, and stop gradient operation are some of the common ways to achieve this asymmetry. Prior work Tian et al. [2021], Jing et al. [2021], Wen and Li [2022] aim to understand the training dynamics of and the role of each of the operation in preventing collapse. We instead focus on the fixed point analyses of the loss functions.

Dimensionality Reduction for GMMs. Spectral Methods are popularly used for dimensionality reduction in gaussian mixture models. Spectral clustering algorithms Sanjeev and Kannan [2001], Vempala and Wang [2004], Achlioptas and McSherry [2005], Kannan et al. [2009], Brubaker and Vempala [2008] pair these spectral methods with standard clustering algorithms (e.g. K-Means) in the low dimensional space. Since the error bounds of these methods vary as square root of the ambient dimension, spectral clustering following the two step process leads to lower clustering error than clustering in the original space itself.

Our work does not focus on state-of-the-art methods for dimensionality reduction for Gaussian mixtures, but instead leverages the problem of dimensionality reduction to analyze self-supervised learning. Specifically, we aim to analyze the role of augmentations/positives in this setup.

3 Problem Setup

We consider data distributions following a Gaussian mixture model (GMM). Intuitively, each mixture component in GMM represents a class in data.

Definition 3.1 (SharedGMM). A *Shared Covariance Gaussian Mixture Model* parameterized by $\{w_k, \boldsymbol{\mu}_k, \boldsymbol{\Sigma}\}_{k \in [K]}$ is defined as the probability distribution $F = \sum_{k \in [K]} w_k \mathcal{N}(\boldsymbol{\mu}_k, \boldsymbol{\Sigma})$ where $\{\boldsymbol{\mu}_k\}_{k \in [K]}$ are the means and $\boldsymbol{\Sigma} \in \mathbb{S}_{++}^d$ is the positive definite covariance matrix shared by the components. w_k are the positive mixture weights summing to one.

Task Formulation. We consider the task of learning a “good” representation function $f(\cdot)$ for points \mathbf{x} drawn from a data distribution. Informally, such a function should map the data onto a lower-dimensional subspace while preserving the class information. For tractability, we restrict f to the class of linear mappings; $\mathbf{x} \mapsto \mathbf{A}^T \mathbf{x}$, where $\mathbf{A} \in \mathbb{R}^{d \times r}$. In this setup, we will show that self-supervised methods can learn the optimal mapping for this task. The standard approach for learning such a mapping is using spectral algorithms Kannan et al. [2009] (See Sec 4.2 for details). We compare and contrast our results for self-supervised methods to well-known results for spectral methods.

Spectral vs Self-supervised Methods. Our results show that self-supervised methods are “better” than spectral methods. We highlight two key points which contribute to the better performance of self-supervised methods. First, spectral methods learn the linear mappings assuming as input a dataset of points, i.e., $\mathbf{x} \sim \mathcal{D}$. In comparison, self-supervised methods operate on input data given as pairs i.e. $(\mathbf{x}, \hat{\mathbf{x}}) \sim \mathcal{D}_{\text{pair}}$ where \mathbf{x} and $\hat{\mathbf{x}}$ are considered to be *similar*. Second, their optimization problems differ in their target objectives. While spectral objectives find the *best-fit* subspace explaining maximum data variance, self-supervised objectives are based on the principle of bringing mappings of similar point closer (in conjunction with a loss-specific regularizer).

$$\begin{aligned} \mathcal{L}_{\text{spectral}}(\mathbf{A}; \mathcal{D}) &= \underbrace{- \|\mathbf{A}^T \mathbf{x}\|^2}_{\text{(negative) explained variance/best fit}} \\ \mathcal{L}_{\text{selfsup}}(\mathbf{A}; \mathcal{D}_{\text{pair}}) &= - \underbrace{(\mathbf{A}^T \mathbf{x})^T \mathbf{A}^T \hat{\mathbf{x}}}_{\text{attractive term}} + \underbrace{\mathcal{R}(\mathbf{x})}_{\text{regularization}} \end{aligned}$$

We elaborate on these differences in more detail in Sec 5.

3.1 Linear Dimensionality Reduction (LDR)

We direct the reader’s attention to the similarity between our task and linear dimensionality reduction (LDR) for Gaussian mixtures. Framing our task as linear dimensionality reduction allows us to establish a quantitative measure of comparison between mappings learned by spectral ($\mathbf{A}_{\text{spectral}}$) and self-supervised methods ($\mathbf{A}_{\text{selfsup}}$).

For a SharedGMM, we denote it’s “intra-component” variance (i.e. variance within a component) by $\boldsymbol{\Sigma}$ and it’s “inter-component” variance (i.e. the distance between components) by $\sum_k w_k \boldsymbol{\mu}_k \boldsymbol{\mu}_k^T$ (following Fukunaga [2013]). A GMM having a low intra-component variance and a high inter-component variance is said to be *well-separated*. LDR aims to map high dimensional GMMs into well-separated low dimensional GMMs. Fisher discriminant Fukunaga [2013] evaluates the performance of such mappings.

	SVD Projection	Contrastive Learning
Data	Single point $\mathbf{x} \sim F$	Pair of points $(\mathbf{x}, \hat{\mathbf{x}}) \sim \hat{F}$
Objective	Maximize data variance	Min. intra-component variance Max. inter-component variance
Fisher-optimality	Spherical GMMs	Shared Covariance GMMs

Table 1: We highlight the differences between classic SVD-based linear dimensionality reduction paradigm and our self-supervised (contrastive) learning-inspired problem setting.

Definition 3.2 (Fisher Discriminant). Suppose a SharedGMM (Def 3.1) parameterized by $\{w_k, \boldsymbol{\mu}_k, \boldsymbol{\Sigma}\}_{k \in [K]}$. Then, the *fisher discriminant* $J(\mathbf{A})$ for a mapping \mathbf{A} (mapping the SharedGMM) is defined as:

$$J(\mathbf{A}) = \text{Tr} \left(\left[\mathbf{A}^T \boldsymbol{\Sigma} \mathbf{A} \right]^{-1} \left[\mathbf{A}^T \left(\sum_k w_k \boldsymbol{\mu}_k \boldsymbol{\mu}_k^T \right) \mathbf{A} \right] \right)$$

Note that $\mathbf{A}^T \boldsymbol{\Sigma} \mathbf{A}$ and $\mathbf{A}^T \left(\sum_k w_k \boldsymbol{\mu}_k \boldsymbol{\mu}_k^T \right) \mathbf{A}$ denote the intra-component and the inter-component variances respectively, *after* the projection operation via \mathbf{A} . Thus, the Fisher discriminant measures the ratio of inter-component to intra-component variances *after* projection.

Remark 3.3. While $J(\mathbf{A})$ is defined in terms of \mathbf{A} , its value is solely a function of $\text{Col}(\mathbf{A})$, i.e. the column space of \mathbf{A} . We hence use the mapping matrix \mathbf{A} and projection subspace $\text{Col}(\mathbf{A})$ interchangeably in our discussion.

A “favorable” mapping \mathbf{A} will have a high value of the Fisher discriminant $J(\mathbf{A})$. Hence, *the Fisher discriminant J serves as the quantitative metric for evaluating $\mathbf{A}_{\text{spectral}}$ and $\mathbf{A}_{\text{selfsup}}$.*

4 Fisher Subspace and Spectral Methods

4.1 Fisher Subspace

It is known that for any target dimension r , the mapping having the top r eigenvectors of $\boldsymbol{\Sigma}^{-1} \left(\sum_k w_k \boldsymbol{\mu}_k \boldsymbol{\mu}_k^T \right)$ as its columns, maximizes the Fisher discriminant. We can also deduce that for any two mappings \mathbf{A}_1 and \mathbf{A}_2 such that $\text{Col}(\mathbf{A}_1) \subseteq \text{Col}(\mathbf{A}_2)$, we have $J(\mathbf{A}_1) \leq J(\mathbf{A}_2)$, i.e., $J(\cdot)$ is monotonic in the subspace of the matrix. Based on this observation, we will have the following definition, which is fundamental in *quantifying the optimality of projections* learned by different methods.

Definition 4.1 (Fisher Subspace). Given a SharedGMM (Def 3.1) parameterized by $\{w_k, \boldsymbol{\mu}_k, \boldsymbol{\Sigma}\}_{k \in [K]}$, its *Fisher subspace* Fukunaga [2013], denoted by S_F , is the smallest subspace that achieves the maximum Fisher discriminant, which is given by:

$$S_F = \text{Span}(\{\boldsymbol{\Sigma}^{-1} \boldsymbol{\mu}_k\}_{k \in [K]}) \quad (1)$$

Class Preserving Subspace. Additionally, we use a unique property Fukunaga [2013] of the Fisher subspace; it is the smallest subspace preserving the class posterior probabilities for Gaussian mixtures with shared covariance.

Lemma 4.2. Let $\{w_k, \boldsymbol{\mu}_k, \boldsymbol{\Sigma}\}_{k \in [K]}$ be a SharedGMM and $\Pr(z = k | \mathbf{x})$ be the posterior probability of \mathbf{x} being drawn from the component z . Let S_F be the mixture’s Fisher subspace and \mathbf{A}_F be a projection matrix such that $\text{Col}(\mathbf{A}_F) = S_F$. Then for any $\mathbf{x} \sim F$,

$$\Pr(z = k | \mathbf{x}) = \Pr(z = k | \mathbf{A}_F^T \mathbf{x}) \quad \forall k \in [K]$$

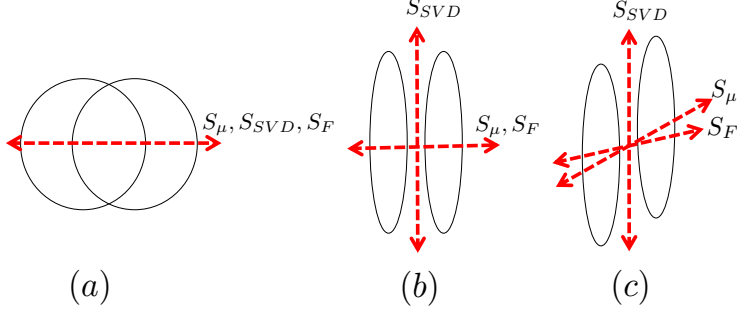


Figure 1: (a) For spherical Gaussians, S_{SVD} and S_F overlap and hence projection onto S_{SVD} leads to *well separated* GMM. (b) (Parallel Pancakes) For general non-spherical Gaussians, large variance in some direction leads to $S_{SVD} \neq S_F$. Hence, projection onto S_{SVD} leads to mode collapse. (c) (Shifted Parallel Pancakes) Mean subspace S_μ does not always coincide with S_F .

Crucially, this property implies that projecting a GMM onto its Fisher subspace will not result in mode collapse or erroneous mode merging. Moreover, any clustering algorithm operating in the lower dimensional subspace will observe the same class probabilities as in the original space. Owing to its properties of maximizing the ratio of inter to intra-component variances and preservation of class probabilities (i.e., index of underlying component), we argue that *Fisher subspace is the optimal subspace for projection*, particularly for the class of shared covariance GMMs.

4.2 Spectral Dimensionality Reduction : SVD-subspace

Spectral methods Kannan et al. [2009] are the standard methods for LDR. They are (generally) based on the principle of finding the best-fit subspace which maximally explains the data. This subspace is given by the *top singular vectors of data covariance*.

Definition 4.3. The r -dimensional *SVD subspace* Vempala and Wang [2004] $S_{SVD}^{(r)}$ for a GMM F is described as the top r left singular vectors of $\mathbb{E}_{\mathbf{x} \sim F}[\mathbf{x}\mathbf{x}^T]$.

A vanilla spectral dimensionality reduction method hence projects the data points onto the r -dimensional SVD subspace. Kannan et al. [2009] proved that for *spherical* GMMs (i.e. $\Sigma = \mathbf{I}$), SVD subspace is equal to the mean subspace $S_\mu = \text{Span}(\mu)$. Moreover, using Eqn 1 we can derive that $S_F = S_\mu = S_{SVD}$. Hence, projection onto the SVD subspace is the optimal dimensionality reduction method for spherical GMMs.

4.3 Parallel Pancakes

While SVD-subspace projection is known to be optimal for spherical GMMs, it is easy to construct examples where spectral methods fail. Intuitively, spectral methods aim to maximally explain the data. This objective leads to “bad” projections when the variance in certain directions is more than the separation between the means, for which we introduce the “parallel pancakes” example Kannan et al. [2009]. Consider a two component GMM that resembles “parallel pancakes”, i.e., the two Gaussians are narrow and separated along one direction, and spherical in all other directions (see Fig 1). The two dimensional SVD subspace for this GMM is given by a plane parallel to the pancakes. The Fisher subspace however, is the plane *passing through the means*; in formal terms $S_{SVD} \not\subset S_F$. In fact, the SVD subspace has the *smallest* Fisher discriminant among all two-dimensional subspaces, and hence, is worse than projection onto a random plane. Finding the optimal low dimensional

space for non-spherical GMMs is known to be a non-trivial Brubaker and Vempala [2008], Kannan et al. [2009].

5 Self-Supervised Learning in Gaussian Mixture Models

We analyze solving the dimensionality reduction task for GMMs with two popular self-supervised methods, namely SimCLR Chen et al. [2020a] and SimSiam Chen and He [2021]. Both methods build on using augmentation pairs, but differ in their optimization objective (specifically how they regularize). We show that both these (differing) objectives are able to effectively leverage the augmentations and learn mappings onto the (optimal) Fisher subspace.

5.1 Augmentation-enabled Distribution

We define the augmentation of a point \mathbf{x} to be an independent sample from the mixture distribution with a *bias* towards the underlying component of \mathbf{x} . The bias implies that if \mathbf{x} is sampled from a component z , then its augmentation, on average, is more likely to be sampled from the same component z . Mathematically, we have :

Definition 5.1 (Augmentation-enabled Distribution (AeD)). For a SharedGMM F parameterized by $\{w_k, \boldsymbol{\mu}_k, \boldsymbol{\Sigma}\}_{k \in [K]}$, we define its *Augmentation-enabled Distribution* \hat{F} , parameterized by $\{w_k, \boldsymbol{\mu}_k, \boldsymbol{\Sigma}, \delta\}_{k \in [K]}$ as

$$\begin{aligned} \hat{F} = & \delta \sum_{k \in [K]} w_k \left(\mathcal{N}(\boldsymbol{\mu}_k, \boldsymbol{\Sigma}) \times \mathcal{N}(\boldsymbol{\mu}_k, \boldsymbol{\Sigma}) \right) \\ & + (1 - \delta) \left(\sum_{k \in [K]} w_k \mathcal{N}(\boldsymbol{\mu}_k, \boldsymbol{\Sigma}) \times \sum_{k' \in [K]} w_{k'} \mathcal{N}(\boldsymbol{\mu}_{k'}, \boldsymbol{\Sigma}) \right) \end{aligned}$$

To elucidate, augmentation-enabled distribution (AeD) returns a pair of points $(\mathbf{x}, \hat{\mathbf{x}}) \sim \hat{F}$ in a two-step process. We first flip a coin with bias δ . Based on the coin flip, we either sample twice from the same component or sample from a possibly different components (chosen with probability w_k). The bias of the coin δ controls the correlation between \mathbf{x} and $\hat{\mathbf{x}}$). For $\delta = 0$, \mathbf{x} and $\hat{\mathbf{x}}$ are independent samples from F , while for $\delta = 1$, \mathbf{x} and $\hat{\mathbf{x}}$ are always from the same component. The definition ensures that the marginal of both \mathbf{x} and $\hat{\mathbf{x}}$ are equal to F for any δ .

Connection to Linear Discriminant Analysis (LDA). LDA Fukunaga [2013] is a *supervised* LDR method that leverages the class information to learn the subspace where the data distribution conditioned on the class label (i.e. the underlying component’s index) is maximally separated (see Suppl H). We highlight that assuming AeD (Def. 5.1) is strictly weaker than assuming a *labeled* dataset. We show that this condition (i.e. access to Augmentation-enabled Distribution) is enough for learning the Fisher subspace and gives similar performance to supervised LDR methods.

5.2 Optimization Objective

InfoNCE loss Oord et al. [2018] is popularly used in contrastive learning methods (like SimCLR). InfoNCE loss aims to learn representations such that a point is close to its augmentation, but far

apart from everything else in the representation space. Concretely, for linear mappings we have

$$\begin{aligned}\mathcal{L}_{\text{Info}}(\mathbf{A}) &= -\mathbb{E}_{(\mathbf{x}, \hat{\mathbf{x}}) \sim \hat{F}} \left[(\mathbf{A}^T \mathbf{x})^T \mathbf{A}^T \hat{\mathbf{x}} \right] \\ &+ \mathbb{E}_{\mathbf{x} \sim F} \left[\log \left(\mathbb{E}_{\tilde{\mathbf{x}} \sim F} \left[\exp ((\mathbf{A}^T \mathbf{x})^T \mathbf{A}^T \tilde{\mathbf{x}}) \right] \right) \right]\end{aligned}\tag{2}$$

where $(\mathbf{x}, \hat{\mathbf{x}}) \sim \hat{F}$ is a sample from AeD (Def 5.1). $\mathbf{x} \sim F$ and $\tilde{\mathbf{x}} \sim F$ are independent draws from the mixture distribution (equivalently $(\mathbf{x}, \cdot) \sim \hat{F}$). The attractive term (i.e. the first term) keeps \mathbf{x} and $\hat{\mathbf{x}}$ close by maximizing their dot product, while regularization term penalizes “proximity” to random samples. Intuitively, the first term in InfoNCE loss aims to increase the inter-component variance while the second term aims to decrease data variance (and hence intra-component variance).

SimSiam Loss Chen and He [2021] is another popular self-supervised loss “without negatives”.

$$-\mathbb{E}_{(\mathbf{x}, \hat{\mathbf{x}}) \sim \hat{F}} \left[\left(\frac{\mathbf{A}_p^T \mathbf{A}^T \mathbf{x}}{\|\mathbf{A}_p^T \mathbf{A}^T \mathbf{x}\|_2} \right)^T \text{StopGrad} \left(\frac{\mathbf{A}^T \hat{\mathbf{x}}}{\|\mathbf{A}^T \hat{\mathbf{x}}\|_2} \right) \right]$$

Note that it only requires augmentations (from \hat{F}) and doesn’t use random samples/negatives (i.e., $\tilde{\mathbf{x}} \sim F$ in Eqn 2). The loss is parameterized by two matrices : \mathbf{A} (the mapping) and \mathbf{A}_p (an additional linear mapping not utilized for projection). The loss also includes a StopGrad operation, which zeros out the gradients flowing through it. For SimSiam, it is trivial to observe that it allows for a collapsing solution (i.e., mapping all points onto the same vector). Prior work Tian et al. [2021], Jing et al. [2021], Wen and Li [2022] has argued that \mathbf{A}_p and StopGrad play a crucial role in the training dynamics, preventing the occurrence of collapse. Our goal is to analyze the fixed point of this loss function. To do so, we introduce some simplifying assumptions and examine a modified SimSiam loss:

$$\begin{aligned}\mathcal{L}_{\text{Siam}}(\mathbf{A}) &= -\mathbb{E}_{(\mathbf{x}, \hat{\mathbf{x}}) \sim \hat{F}} \left[(\mathbf{A}^T \mathbf{x})^T \mathbf{A}^T \hat{\mathbf{x}} \right] \\ &+ \xi \mathbb{E}_{\mathbf{x} \sim F} \left[\|\mathbf{A}^T \mathbf{x}\|^2 \right]\end{aligned}\tag{3}$$

We remove the StopGrad operation and set the prediction head (i.e. \mathbf{A}_p) to \mathbf{I} . We also trade the normalization term with a regularization term weighted by ξ . The attractive term in SimSiam behaves similar to InfoNCE loss, while the regularization term penalizes the norm of the projected points. The loss scales linearly with the squared norm of the matrix \mathbf{A} ; we impose a norm constraint when optimizing for \mathbf{A} .

Contrasting to best-fit objective We have established that spectral methods (specifically, SVD-subspace projection) learn projection matrices that induces maximal variance in the projected space;

$$\underset{\{\mathbf{A} \in \mathbb{R}^{d \times r}: \mathbf{A}^T \mathbf{A} = \mathbf{I}\}}{\text{argmax}} \mathbb{E}_{\mathbf{x} \sim F} [\|\mathbf{A}^T \mathbf{x}\|^2] \tag{4}$$

Informally, this objective is orthogonal to the goal of dimensionality reduction. Recall that our dimensionality reduction definition aims to find a projection space such that intra-component variance is *low* while inter-component variance is *high*. We can observe that optimizing a self-supervised objective serves as a better proxy for dimensionality reduction. We will now formalize our claim.

5.3 Main theorem

Equipped with the definitions of augmentations (Def 5.1) and the optimization objectives (Eqn 2, 3), we prove that we can find the optimal projection matrix for the class of SharedGMMs (Def. 3.1).

Theorem 5.2. *Suppose F is a SharedGMM parameterized by $\{w_k, \boldsymbol{\mu}_k, \boldsymbol{\Sigma}\}_{k \in [K]}$ and \hat{F} is its Augmentation-enabled Distribution with bias δ . Let S_F be the Fisher subspace (Eqn 1) of F . Denote λ_{\min} as the minimum non-zero eigenvalue of $\boldsymbol{\Sigma}^{-\frac{1}{2}} \sum_k w_k \boldsymbol{\mu}_k \boldsymbol{\mu}_k^T \boldsymbol{\Sigma}^{-\frac{1}{2}}$ and*

$$\mathbf{A}_{\text{Info}} = \underset{\mathbf{A} \in \mathbb{R}^{d \times r}}{\operatorname{argmin}} \mathcal{L}_{\text{Info}}(\mathbf{A}), \quad \mathbf{A}_{\text{Siam}} = \underset{\substack{\mathbf{A} \in \mathbb{R}^{d \times r} \\ \|\mathbf{A}\|_2 \leq 1}}{\operatorname{argmin}} \mathcal{L}_{\text{Siam}}(\mathbf{A})$$

Then for some $r \geq K$, $S_{\text{Info}} \triangleq \text{Col}(\mathbf{A}_{\text{Info}})$, $S_{\text{Siam}} \triangleq \text{Col}(\mathbf{A}_{\text{Siam}})$, we have :

- $S_{\text{Info}} \subseteq S_F$. If $\delta = 1$, then $S_{\text{Info}} = S_F$
- $S_{\text{Siam}} \subseteq S_F$. If $0 < \xi < \frac{\delta \lambda_{\min}}{1 + \lambda_{\min}}$, then $S_{\text{Siam}} = S_F$

Remark 5.3. Thm 5.2 states that access to Augmentation-enabled Distribution augmentations is **provably sufficient** for learning the Fisher subspace for SharedGMMs. The result implies that class labels — typically assumed by supervised LDR methods like LDA — are not necessary.

The proof of Thm 5.2 can be found in Suppl C, D. For population setting, self-supervised methods learn mapping onto a subset of the Fisher space. This implies that the projected points do not capture any *noise* and only contain a subset of the useful *features*. Note that spectral methods do not have any guarantees of this form (See Sec 4.3 for discussion).

The theorem also states if we have perfect augmentations for InfoNCE loss, i.e. $\delta = 1$, we cover *all directions* in the Fisher space and learn it exactly. The equivalence is true for SimSiam loss when the regularization coefficient ξ is upper bounded appropriately. Importantly, this precludes learning of the collapsing solution for SimSiam loss. Under these conditions, we learn *the same subspace* as completely *supervised* dimensionality reduction methods.

Technical Difficulties Although we do not provide a proof for $S_{\text{Info}} = S_F$ when $0 < \delta < 1$, we conjecture that the same is true, for which we include an empirical discussion in Sec 7. The results in Fig 4a suggest that $S_{\text{Info}} = S_F$ even for $\delta < 1$, and we leave the concrete analysis in this value range as future work. Additionally, we do not have an exact characterization of InfoNCE solution (we characterize just the column space of \mathbf{A}_{Info}). Our empirical results show that the mapped points are well-separated compared to a projection onto the Fisher subspace (see Fig 2d). Furthermore, while we prove that both contrastive and non-contrastive objectives learn the same subspace, further investigation is required for their direct comparison. In Suppl F we provide an example where \mathbf{A}_{Info} is strictly better than $\mathbf{A}_{\text{SimSiam}}$ (for $r < K$). We also present an empirical study on the effect of r in Section 7 (see Figure 4c).

6 Multi-Modal Gaussian Mixtures and Self-Supervised Learning

In the previous section, we considered the setup in which a point and its augmentation follow the same distribution. This is a sound assumption for methods like SimCLR and SimSiam where augmentations of points (i.e. images) are defined by transformations (e.g., cropping, color jittering etc) on the image.

This assumption may not hold in general. Text embeddings models like DPR Karpukhin et al. [2020] or image-text embedding models like CLIP Radford et al. [2021] consider input samples as a pair of points following (possibly) different distribution. For instance, each sample could be a pair of an image with its corresponding caption (for CLIP) or a search query with a relevant document that answers the query (for DPR). The objective of methods considering multi-modal data is to learn a joint representation space for both the modalities such that representations of points in a pair are close, while being far from random draws. These joint representations can be used downstream for finding similarities between points (belonging to different modalities). Surprisingly, representations learned for each modality are competitive to fully supervised representations Radford et al. [2021]. Our goal is to theoretically analyze the representations learned by multi-modal models, specifically the CLIP model.

CLIP Gaussian Mixtures (CLIPGMM) We define CLIPGMM to capture multi-modal data in a theory-friendly setting.

Definition 6.1. (CLIPGMM) A *CLIP Gaussian mixture* (CLIPGMM) is defined as the probability distribution $F_{\text{clip}} = \sum_{k \in [K]} w_k \mathcal{N}(\boldsymbol{\mu}_{V,k}, \boldsymbol{\Sigma}_V) \times \mathcal{N}(\boldsymbol{\mu}_{T,k}, \boldsymbol{\Sigma}_T)$ where w_k are the mixture weights, $\{\boldsymbol{\mu}_{V,k}\}_{k \in [K]}$, $\boldsymbol{\Sigma}_V$ and $\{\boldsymbol{\mu}_{T,k}\}_{k \in [K]}$, $\boldsymbol{\Sigma}_T$ are the parameters for the two coordinate spaces respectively.

CLIPGMM is hence a mixture of product distribution over Gaussians. To elaborate, a sampling $(\mathbf{x}_V, \mathbf{x}_T) \sim F_{\text{clip}}$ is a two step process. We first sample an underlying component index, and then draw independent samples from the component *with the same index* in the respective coordinate space. F_{clip} can be used to define marginal distribution over each coordinate space; $F_V = \sum_{k \in [K]} w_k \mathcal{N}(\boldsymbol{\mu}_{V,k}, \boldsymbol{\Sigma}_V)$. Marginal over T space can be defined similarly.

Problem Setup Following CLIP Radford et al. [2021], we want to learn two different representation functions (one for each modality). We let these functions be linear mappings (say, $\mathbf{A}_V \in \mathbb{R}^{d_1 \times r}$, $\mathbf{A}_T \in \mathbb{R}^{d_2 \times r}$). Recall that optimal mapping matrices for each coordinate space would have their column space equal to the Fisher subspace for the marginal distributions F_V, F_T . We show CLIP learns a mapping onto the subset of the Fisher subspace by jointly optimizing over multi-modal pairs, without augmentations.

6.1 Optimization Objective

We now formalize the CLIP InfoNCE loss Radford et al. [2021]. Concretely, let the representation of a sample $(\mathbf{x}_V, \mathbf{x}_T)$ be given by $(\mathbf{A}_V^T \mathbf{x}_V, \mathbf{A}_T^T \mathbf{x}_T)$, where $\mathbf{A}_V, \mathbf{A}_T$ are the mappings for the two coordinate spaces. Then,

$$\begin{aligned} \mathcal{L}_{\text{clip}}(\mathbf{A}_V, \mathbf{A}_T) = & - \mathbb{E}_{(\mathbf{x}_V, \mathbf{x}_T) \sim F_{\text{clip}}} \left[(\mathbf{A}_T^T \mathbf{x}_T)^T \mathbf{A}_V^T \mathbf{x}_V \right] \\ & + \mathbb{E}_{\mathbf{x}_T \sim F_T} \left[\log \left(\mathbb{E}_{\mathbf{x}_V \sim F_V} \left[\exp ((\mathbf{A}_T^T \mathbf{x}_T)^T \mathbf{A}_V^T \mathbf{x}_V) \right] \right) \right] \end{aligned} \quad (5)$$

Each coordinate space serves as an "augmentation" for the other coordinate space. Similar to InfoNCE, CLIP InfoNCE attract representations of \mathbf{x}_V and \mathbf{x}_T through first term, while regularizing with the Log-Sum-Exp term.

6.2 Results

Our main result for CLIPGMM states that we can learn a subset of Fisher subspace for the constituent modalities by minimizing the CLIP InfoNCE loss. Concretely,

Theorem 6.2. *Suppose $\{w_k, \mu_{V,k}, \mu_{T,k}, \Sigma_V, \Sigma_T\}_{k \in [K]}$ is a CLIPGMM (Def 6.1). Let the Fisher subspace of F_V be $S_{V,F}$ and F_T be $S_{T,F}$. Denote $\mathbf{A}_V^*, \mathbf{A}_T^*$ as the optimal solution of the CLIP InfoNCE loss (Eqn 5), i.e.,*

$$\mathbf{A}_V^*, \mathbf{A}_T^* = \underset{\substack{\mathbf{A}_V \in \mathbb{R}^{d_1 \times r} \\ \mathbf{A}_T \in \mathbb{R}^{d_2 \times r}}}{\operatorname{argmin}} \mathcal{L}_{\text{clip}}(\mathbf{A}_V, \mathbf{A}_T)$$

For any $r \geq K$, let $S_{V,\text{clip}} = \text{Col}(\mathbf{A}_V^*)$ and $S_{T,\text{clip}} = \text{Col}(\mathbf{A}_T^*)$. Then, $S_{V,\text{clip}} \subseteq S_{V,F}$ and $S_{T,\text{clip}} \subseteq S_{T,F}$.

The proof of Thm 6.2 can be found in Suppl E. In simple words, we learn the subset of the Fisher subspace instead of the *exact space* and hence is *weaker* result than the single-modal setting with augmentations. The result still shows that self-supervised learning for multi-modal data is *better than spectral methods*, since we are always a subset of S_F , which doesn't hold for spectral methods (Fig 1).

The reason it is weaker than the single-modal GMM, however, is due to the fact that the means in the two spaces can vary arbitrarily. Hence, one can come up with adversarial set of means and covariances such that particular directions in the Fisher subspace (of either F_V or F_T) doesn't contribute to the inter-component distance and hence is not learned by the CLIP InfoNCE objective. For certain special configuration of model parameters such as $\Sigma_T^{-\frac{1}{2}} \mu_{T,k} = \Sigma_V^{-\frac{1}{2}} \mu_{V,k}$, we can achieve $S_{T,\text{clip}} = S_{T,F}$ and $S_{V,\text{clip}} = S_{V,F}$.

7 Synthetic Experiments

We validate our theoretical findings with experiments on synthetic data. We study the effect of noise δ in Augmentation-enabled Distribution and also how the rank r of the projection matrix and condition number of covariance matrix effect the learned representations. Finally we show that apart from learning the optimal projection subspace, self-supervised learning also leads to a "good" scaling within the subspace.

7.1 Setup

We aim to evaluate different representation learning (linear dimensionality reduction) methods for the class of shared covariance GMMs (Eqn 3.1). We adopt a two-step process for evaluating the performance of the methods. The first step is dimensionality reduction with the target method, and the second step is clustering with an out-of-the-box clustering algorithm (i.e. K-Means ¹). We compare the methods based on their clustering performance in the second step.

Metrics Following prior work Jiang et al. [2020] we use Adjusted Rank Index (*ARI*) and Adjusted Mutual Information (*AMI*) to measure the quality of a clustering algorithms. We give the ground

¹<https://scikit-learn.org/1.5/modules/generated/sklearn.cluster.KMeans.html>

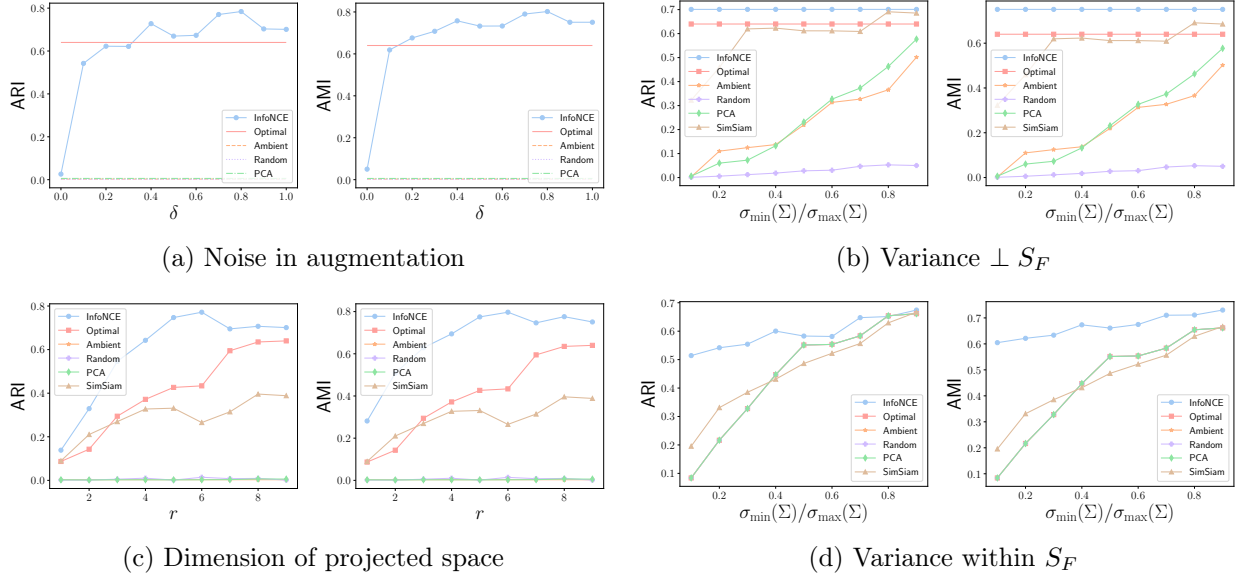


Figure 2: We empirically validate our theoretical findings for four main settings (see Sec 7). Fig (a), shows that self-supervised learning is robust to noise in Augmentation-enabled Distribution . Fig (b), shows that InfoNCE (and SimSiam) are invariant to variance orthogonal to fisher subspace. Fig (c), InfoNCE loss is better than spectral methods for every projection dimension, and Fig (d) shows that InfoNCE loss learns a good scaling within the fisher subspace

truth number of clusters to K-Means as input. ARI and AMI both vary between 0 and 1, with 0 corresponding to random clustering and 1 corresponding to perfect clustering.

Data Generation For all our experiments we consider $K = 10$ equally likely (i.e. $w_i = 1/K$) component mixtures. See Suppl G.1 for details.

Methods We consider four main baselines. 1) *Ambient* is clustering in ambient dimension, i.e. no mapping. 2) *Random* projects onto a random subspace of dimension r . 3) *Optimal* projects onto top r directions in Fisher subspace. 4) *PCA* projects onto the top r principal component of the samples (equivalent to SVD-subspace projection). On top of the baselines we also consider learning the mapping matrix \mathbf{A} using gradient descent with respect to 5) *InfoNCE* loss and 6) *SimSiam* loss. Note that InfoNCE and SimSiam also learn scaling within the subspace (while baselines like PCA *only* project).

7.2 Results

We observe that InfoNCE often performs better than Optimal (i.e. projection onto the Fisher subspace). We interpret that InfoNCE loss learns to *scale* within the subspace leading to better clustering performance (we present plots on ortho-normalized InfoNCE/SimSiam in Suppl G.2). Also observe SimSiam shows a sub-par performance compared to InfoNCE contrary to our theoretical results. We believe this is due the difficulty in optimizing the SimSiam objective (projected gradient descent) compared to InfoNCE.

Effect of noise in augmentations We vary the noise parameter δ for the AeD with everything else held constant. We can see in Fig 4a that InfoNCE is robust to the variation in δ and performs well even for small values of δ .

Effect of variance orthogonal to S_F Here we consider the effect of increasing the variance in directions *orthogonal to the Fisher subspace* (i.e. making the pancake in Fig 1 flatter). We quantify the “flatness” as $\sigma_{\min}(\Sigma)/\sigma_{\max}(\Sigma)$. Fig 4b shows that InfoNCE is (almost) invariant to “flatness”, while PCA and Ambient fail when the variance orthogonal to Fisher subspace is large (i.e. $\sigma_{\min}(\Sigma)/\sigma_{\max}(\Sigma)$ is small).

Effect of projection dimension We vary the dimension of the lower dimensional space that we aim to learn. InfoNCE’s performance increases with increasing r and finally plateaus.

Effect of variance within S_F We also show that InfoNCE learns a “good” scaling within the Fisher subspace. For this, we let the dimension of ambient space equal to the dimension of mean subspace (i.e. $d = K - 1$). We select $K/2 = 5$ orthogonal directions and increase the variance in the subspace spanned by these direction by a factor of $\sigma_{\max}(\Sigma)/\sigma_{\min}(\Sigma)$. Since none of the baselines learn scaling in the subspace (and $d = r = K - 1$), they perform almost the same, while InfoNCE improves.

8 Conclusion and Discussion

We study self-supervised learning in a classic setting of dimensionality reduction for Gaussian Mixture Models. A key idea that enabled this was defining the notion of augmentations and point pairs. We showed that for the problem of dimensionality reduction, *if* given the luxury of augmentations, we can go meaningfully beyond what is possible with completely unsupervised methods. Our main result underline that the contrastive learning paradigm learns the Fisher-optimal subspace for the class of shared-covariance GMMs. For future work, we hope to make use of our novel setting to design new, provable *algorithms* for learning Fisher-optimal subspaces.

Acknowledgments

Ali Kavis is funded in part by the Swiss National Science Foundation (SNSF) under grant number P500PT_217942.

References

Ting Chen, Simon Kornblith, Mohammad Norouzi, and Geoffrey Hinton. A simple framework for contrastive learning of visual representations. In Hal Daumé III and Aarti Singh, editors, *Proceedings of the 37th International Conference on Machine Learning*, volume 119 of *Proceedings of Machine Learning Research*, pages 1597–1607. PMLR, 13–18 Jul 2020a. URL <https://proceedings.mlr.press/v119/chen20j.html>.

Xinlei Chen, Haoqi Fan, Ross Girshick, and Kaiming He. Improved baselines with momentum contrastive learning. *arXiv preprint arXiv:2003.04297*, 2020b.

Vladimir Karpukhin, Barlas Oğuz, Sewon Min, Patrick Lewis, Ledell Wu, Sergey Edunov, Danqi Chen, and Wen-tau Yih. Dense passage retrieval for open-domain question answering. *arXiv preprint arXiv:2004.04906*, 2020.

Alec Radford, Jong Wook Kim, Chris Hallacy, Aditya Ramesh, Gabriel Goh, Sandhini Agarwal, Girish Sastry, Amanda Askell, Pamela Mishkin, Jack Clark, et al. Learning transferable visual models from natural language supervision. In *International conference on machine learning*, pages 8748–8763. PMLR, 2021.

Gautier Izacard, Mathilde Caron, Lucas Hosseini, Sebastian Riedel, Piotr Bojanowski, Armand Joulin, and Edouard Grave. Unsupervised dense information retrieval with contrastive learning. *arXiv preprint arXiv:2112.09118*, 2021.

Sanjeev Arora, Hrishikesh Khandeparkar, Mikhail Khodak, Orestis Plevrakis, and Nikunj Saunshi. A theoretical analysis of contrastive unsupervised representation learning. *arXiv preprint arXiv:1902.09229*, 2019.

Jeff Z HaoChen, Colin Wei, Adrien Gaidon, and Tengyu Ma. Provable guarantees for self-supervised deep learning with spectral contrastive loss. *Advances in Neural Information Processing Systems*, 34:5000–5011, 2021.

Nikunj Saunshi, Jordan Ash, Surbhi Goel, Dipendra Misra, Cyril Zhang, Sanjeev Arora, Sham Kakade, and Akshay Krishnamurthy. Understanding contrastive learning requires incorporating inductive biases. In *International Conference on Machine Learning*, pages 19250–19286. PMLR, 2022.

Jeff Z HaoChen and Tengyu Ma. A theoretical study of inductive biases in contrastive learning. *arXiv preprint arXiv:2211.14699*, 2022.

Jean-Bastien Grill, Florian Strub, Florent Altché, Corentin Tallec, Pierre Richemond, Elena Buchatskaya, Carl Doersch, Bernardo Avila Pires, Zhaohan Guo, Mohammad Gheshlaghi Azar, et al. Bootstrap your own latent-a new approach to self-supervised learning. *Advances in neural information processing systems*, 33:21271–21284, 2020.

Mathilde Caron, Ishan Misra, Julien Mairal, Priya Goyal, Piotr Bojanowski, and Armand Joulin. Unsupervised learning of visual features by contrasting cluster assignments. *Advances in neural information processing systems*, 33:9912–9924, 2020.

Xinlei Chen and Kaiming He. Exploring simple siamese representation learning. In *Proceedings of the IEEE/CVF conference on computer vision and pattern recognition*, pages 15750–15758, 2021.

Xiao Wang, Haoqi Fan, Yuandong Tian, Daisuke Kihara, and Xinlei Chen. On the importance of asymmetry for siamese representation learning. In *Proceedings of the IEEE/CVF conference on computer vision and pattern recognition*, pages 16570–16579, 2022.

Yuandong Tian, Xinlei Chen, and Surya Ganguli. Understanding self-supervised learning dynamics without contrastive pairs. In *International Conference on Machine Learning*, pages 10268–10278. PMLR, 2021.

Li Jing, Pascal Vincent, Yann LeCun, and Yuandong Tian. Understanding dimensional collapse in contrastive self-supervised learning. *arXiv preprint arXiv:2110.09348*, 2021.

Zixin Wen and Yuanzhi Li. The mechanism of prediction head in non-contrastive self-supervised learning. *Advances in Neural Information Processing Systems*, 35:24794–24809, 2022.

Arora Sanjeev and Ravi Kannan. Learning mixtures of arbitrary gaussians. In *Proceedings of the Thirty-Third Annual ACM Symposium on Theory of Computing*, STOC ’01, page 247–257, New York, NY, USA, 2001. Association for Computing Machinery. ISBN 1581133499. doi: 10.1145/380752.380808. URL <https://doi.org/10.1145/380752.380808>.

Santosh Vempala and Grant Wang. A spectral algorithm for learning mixture models. *Journal of Computer and System Sciences*, 68(4):841–860, 2004.

Dimitris Achlioptas and Frank McSherry. On spectral learning of mixtures of distributions. In *International Conference on Computational Learning Theory*, pages 458–469. Springer, 2005.

Ravindran Kannan, Santosh Vempala, et al. Spectral algorithms. *Foundations and Trends® in Theoretical Computer Science*, 4(3–4):157–288, 2009.

S Charles Brubaker and Santosh S Vempala. Isotropic pca and affine-invariant clustering. *Building Bridges: Between Mathematics and Computer Science*, pages 241–281, 2008.

Keinosuke Fukunaga. *Introduction to statistical pattern recognition*. Elsevier, 2013.

Aaron van den Oord, Yazhe Li, and Oriol Vinyals. Representation learning with contrastive predictive coding. *arXiv preprint arXiv:1807.03748*, 2018.

Heinrich Jiang, Jennifer Jang, and Jakub Lacki. Faster dbscan via subsampled similarity queries. *Advances in Neural Information Processing Systems*, 33:22407–22419, 2020.

Appendix

A Additional Lemmas

Lemma A.1. *The function given by $f(\{\mathbf{x}_i\}; \mathbf{c}) = \log(\sum_i \exp(\mathbf{c}^T \mathbf{x}_i))$ where $\{\mathbf{x}_i\}, \mathbf{c} \in \mathbb{R}^d$ is strictly convex in $\mathbf{c} \in \text{Span}(\{\mathbf{x}_i\})$.*

Proof. Using the definition of strict convexity we need to prove that:

$$\begin{aligned} & f(\{\mathbf{x}_i\}; (\lambda \mathbf{c}_1 + (1 - \lambda) \mathbf{c}_2)) \\ & < \lambda f(\{\mathbf{x}_i\}; \mathbf{c}_1) + (1 - \lambda) f(\{\mathbf{x}_i\}; \mathbf{c}_2) \end{aligned}$$

when $\mathbf{c}_1 \neq \mathbf{c}_2$. Taking $\exp(\cdot)$ on both sides :

$$\begin{aligned} & \exp(f(\{\mathbf{x}_i\}; (\lambda \mathbf{c}_1 + (1 - \lambda) \mathbf{c}_2))) \\ & < \exp(\lambda f(\{\mathbf{x}_i\}; \mathbf{c}_1)) \exp((1 - \lambda) f(\{\mathbf{x}_i\}; \mathbf{c}_2)) \end{aligned}$$

Simplifying the LHS we have :

$$\begin{aligned} & \exp(f(\{\mathbf{x}_i\}; (\lambda \mathbf{c}_1 + (1 - \lambda) \mathbf{c}_2))) \\ & = \sum_i \exp((\lambda \mathbf{c}_1 + (1 - \lambda) \mathbf{c}_2)^T \mathbf{x}_i) \\ & = \sum_i \exp(\lambda \mathbf{c}_1^T \mathbf{x}_i) \exp((1 - \lambda) \mathbf{c}_2^T \mathbf{x}_i) \end{aligned}$$

Using Holders inequality ($\sum_i x_i y_i \leq (\sum_i |x_i|^p)^{\frac{1}{p}} (\sum_i |y_i|^q)^{\frac{1}{q}}$, where $\frac{1}{p} + \frac{1}{q} = 1$) with $p = \frac{1}{\lambda}$ and $q = \frac{1}{1-\lambda}$, we have :

$$\begin{aligned} & \sum_i \exp(\lambda \mathbf{c}_1^T \mathbf{x}_i) \exp((1 - \lambda) \mathbf{c}_2^T \mathbf{x}_i) \\ & \leq \left(\sum_i \exp\left(\frac{\lambda \mathbf{c}_1^T \mathbf{x}_i}{\lambda}\right) \right)^\lambda \left(\sum_i \exp\left(\frac{(1 - \lambda) \mathbf{c}_2^T \mathbf{x}_i}{1 - \lambda}\right) \right)^{(1-\lambda)} \\ & = \left(\sum_i \exp(\mathbf{c}_1^T \mathbf{x}_i) \right)^\lambda \left(\sum_i \exp(\mathbf{c}_2^T \mathbf{x}_i) \right)^{(1-\lambda)} \\ & = \exp(\lambda f(\{\mathbf{x}_i\}; \mathbf{c}_1)) \exp((1 - \lambda) f(\{\mathbf{x}_i\}; \mathbf{c}_2)) \end{aligned}$$

Note that Holders equality holds only when $\mathbf{c}_1^T \mathbf{x}_i = \mathbf{c}_2^T \mathbf{x}_i$ for all i . For $\mathbf{c}_1, \mathbf{c}_2 \in \text{Span}\{\mathbf{x}_i\}$, this

equality holds only when $\mathbf{c}_1 = \mathbf{c}_2$. Hence, for $\mathbf{c}_1 \neq \mathbf{c}_2$ we have strict inequality i.e.

$$\begin{aligned} & \sum_i \exp(\lambda \mathbf{c}_1^T \mathbf{x}_i) \exp((1-\lambda) \mathbf{c}_2^T \mathbf{x}_i) \\ & < \left(\sum_i \exp\left(\frac{\lambda \mathbf{c}_1^T \mathbf{x}_i}{\lambda}\right) \right)^\lambda \left(\sum_i \exp\left(\frac{(1-\lambda) \mathbf{c}_2^T \mathbf{x}_i}{1-\lambda}\right) \right)^{(1-\lambda)} \\ & = \exp(\lambda f(\{\mathbf{x}_i\}; \mathbf{c}_1)) \exp((1-\lambda) f(\{\mathbf{x}_i\}; \mathbf{c}_2)) \end{aligned}$$

This gives strict convexity. Hence proved. \square

B Main Proposition

In this section, we state and prove a key proposition which is used to prove our main result (Thm 5.2)

Proposition B.1. *Suppose F parameterized by $\{w_k, \mu_k, I\}_{k \in [K]}$ be a spherical gaussian mixture model (Def ??) and \hat{F} be its augmentation-enabled gaussian mixture with bias δ (Def 5.1). Let S_F be the fisher subspace (Eqn 1) of F and \mathbf{A}^* be the optimal solution of the InfoNCE loss (Eqn 2) :*

$$\mathbf{A}^* = \underset{\mathbf{A} \in \mathbb{R}^{d \times r}}{\operatorname{argmin}} \mathcal{L}(\mathbf{A})$$

Then given $r \geq K$, $\operatorname{Col}(\mathbf{A}^) \subseteq S_F$. Moreover if $\delta = 1$, then $\operatorname{Col}(\mathbf{A}^*) = S_F$.*

We prove the proposition in two parts. In the first part we prove that $\operatorname{Col}(\mathbf{A}^*) \subseteq S_F$ for any $\delta > 0$. In the second part we prove that if $\delta = 1$, then $\operatorname{Col}(\mathbf{A}^*) = S_F$.

B.1 Column space of \mathbf{A} is a subset of Fischer Subspace

We prove that : $\operatorname{Col}(\mathbf{A}^*) \subseteq S_F$ when $\delta > 0$

Proof.

$$(\mathbf{A}^T \mathbf{x})^T (\mathbf{A}^T \mathbf{y}) = \mathbf{x}^T \mathbf{A} \mathbf{A}^T \mathbf{y} = \mathbf{x}^T \mathbf{B} \mathbf{y}$$

, where $\mathbf{B} = \mathbf{A} \mathbf{A}^T$, i.e. \mathbf{B} is positive semi-definite (PSD) matrix of rank r . We substitute into InfoNCE loss to get :

$$\mathcal{L} = -\mathbb{E}_{\mathbf{x}, \hat{\mathbf{x}}}[\mathbf{x}^T \mathbf{B} \hat{\mathbf{x}}] + \mathbb{E}_{\mathbf{x}}[\log(\mathbb{E}_{\tilde{\mathbf{x}}}[\exp(\mathbf{x}^T \mathbf{B} \tilde{\mathbf{x}})])]$$

We relax the rank-constraint on \mathbf{B} throughout the proof. We show that rank of our optimal solution $\mathbf{B}^* \leq K$ which satisfies the rank constraint implicitly (as $K \leq r$).

Note : The above loss function is strictly convex in \mathbf{B} (using Lemma A.1) and the minimization of is over a convex set (i.e. set of $\mathbf{B} \in \mathbb{S}_+^d$).

Let \mathbf{B}^* be the optimal solution. Denote the eigendecomposition of \mathbf{B}^* as $\mathbf{U} \mathbf{\Lambda} \mathbf{U}^T$, where $\mathbf{\Lambda} \succeq 0$ (as $\mathbf{B} \succeq 0$) and \mathbf{U} is a unitary matrix. Equivalently :

$$\mathbf{B}^* = \sum_i \lambda_i \mathbf{u}_i \mathbf{u}_i^T \tag{6}$$

where \mathbf{u}_i are columns of \mathbf{U} . Consider the indices where the eigenvalue $\lambda_i > 0$ as \mathcal{I} . The solution \mathbf{A}^* is hence $[\sqrt{\lambda_i} \mathbf{u}_i]_{i \in \mathcal{I}}$. We aim to show that $\text{Col}(\mathbf{A}^*) = \text{Span}\{\mathbf{u}_i\}_{i \in \mathcal{I}} \subseteq \text{Span}\{\boldsymbol{\mu}_k\}_{k \in [K]}$.

The condition $\text{Span}\{\mathbf{u}_i\}_{i \in \mathcal{I}} \subseteq \text{Span}\{\boldsymbol{\mu}_k\}_{k \in [K]}$ implicitly implies that rank of $\mathbf{B}^* \leq K$. This follows because there can't be more than K orthogonal vectors (i.e. columns of U) in a subspace of dimension K (as there are only K means spanning the subspace).

Suppose the condition is not true. Then there exists a unit vector \mathbf{v} , such that $\mathbf{v}^T \boldsymbol{\mu}_k = 0$ for all $k \in [K]$ and $\mathbf{v}^T \mathbf{u}_i \neq 0$ for some i where $\lambda_i > 0$.

We construct a new matrix $\bar{\mathbf{U}}$, whose columns are reflection of \mathbf{U} through the plane with normal vector \mathbf{v} given by $\mathbf{R} = \mathbf{I} - 2\mathbf{v}\mathbf{v}^T$. The reflection matrix is defined such that $\mathbf{R}\boldsymbol{\mu}_k = \mathbf{R}^T\boldsymbol{\mu}_k = \boldsymbol{\mu}_k$. Define $\bar{\mathbf{B}}$ from the constructed $\bar{\mathbf{U}}$.

$$\begin{aligned}\bar{\mathbf{U}} &= \mathbf{R}\mathbf{U} = (\mathbf{I} - 2\mathbf{v}\mathbf{v}^T)\mathbf{U} \\ \bar{\mathbf{B}} &= \bar{\mathbf{U}}\boldsymbol{\Lambda}\bar{\mathbf{U}}^T = \mathbf{R}\mathbf{B}^*\mathbf{R}^T\end{aligned}$$

$\bar{\mathbf{B}} \neq \mathbf{B}$. $\bar{\mathbf{U}} \neq \mathbf{U}$ is still a unitary matrix (product of unitary matrices), is identical to \mathbf{U} in $\text{Span}\{\boldsymbol{\mu}_k\}_{k \in [K]}$

$$\begin{aligned}\bar{\mathbf{U}}^T \bar{\mathbf{U}} &= \mathbf{U}^T \mathbf{R}^T \mathbf{R} \mathbf{U} = \mathbf{U}^T \mathbf{U} = \mathbf{I} \\ \bar{\mathbf{U}}^T \boldsymbol{\mu}_k &= \mathbf{U}^T \mathbf{R}^T \boldsymbol{\mu}_k = \mathbf{U}^T \boldsymbol{\mu}_k \\ \bar{\mathbf{U}} \boldsymbol{\mu}_k &= \mathbf{U} \mathbf{R} \boldsymbol{\mu}_k = \mathbf{U} \boldsymbol{\mu}_k\end{aligned}$$

The first term in the loss \mathcal{L} at \mathbf{B}^* can be simplified as

$$\begin{aligned}\mathbb{E}_{\mathbf{x}, \hat{\mathbf{x}}}[\mathbf{x}^T \mathbf{B}^* \hat{\mathbf{x}}] &= \mathbb{E}_{\mathbf{x}, \hat{\mathbf{x}}}[\langle \mathbf{x} \hat{\mathbf{x}}^T, \mathbf{B}^* \rangle] \\ &= \langle \mathbb{E}_{\mathbf{x}, \hat{\mathbf{x}}}[\mathbf{x} \hat{\mathbf{x}}^T], \mathbf{B}^* \rangle \\ &= \langle \sum_k w_k \boldsymbol{\mu}_k (\delta \boldsymbol{\mu}_k + (1 - \delta) (\sum_j w_j \boldsymbol{\mu}_j))^T, \mathbf{B}^* \rangle \\ &= \langle \delta \sum_k w_k \boldsymbol{\mu}_k \boldsymbol{\mu}_k^T + (1 - \delta) (\sum_k w_k \boldsymbol{\mu}_k) (\sum_j w_j \boldsymbol{\mu}_j)^T, \mathbf{B}^* \rangle\end{aligned}$$

This is where we use the fact that the augmentation is generated from the augmentation oracle.

We can now see that

$$\begin{aligned}
& \mathbb{E}_{\mathbf{x}, \hat{\mathbf{x}}}[\mathbf{x}^T \bar{\mathbf{B}} \hat{\mathbf{x}}] \\
&= \langle \delta \sum_k w_k \boldsymbol{\mu}_k \boldsymbol{\mu}_k^T + (1-\delta) \left(\sum_k w_k \boldsymbol{\mu}_k \right) \left(\sum_j w_j \boldsymbol{\mu}_j \right)^T, \bar{\mathbf{B}} \rangle \\
&= \langle \delta \sum_k w_k \boldsymbol{\mu}_k \boldsymbol{\mu}_k^T + (1-\delta) \left(\sum_k w_k \boldsymbol{\mu}_k \right) \left(\sum_j w_j \boldsymbol{\mu}_j \right)^T, \mathbf{R} \mathbf{B} \mathbf{R}^T \rangle \\
&= \langle \delta \sum_k w_k \mathbf{R}^T \boldsymbol{\mu}_k \boldsymbol{\mu}_k^T \mathbf{R} + \\
& \quad (1-\delta) \left(\sum_k w_k \mathbf{R}^T \boldsymbol{\mu}_k \right) \left(\sum_j w_j \mathbf{R}^T \boldsymbol{\mu}_j \right)^T, \mathbf{B}^* \rangle \\
&= \langle \delta \sum_k w_k \boldsymbol{\mu}_k \boldsymbol{\mu}_k^T + (1-\delta) \left(\sum_k w_k \boldsymbol{\mu}_k \right) \left(\sum_j w_j \boldsymbol{\mu}_j \right)^T, \mathbf{B}^* \rangle \\
&= \mathbb{E}_{\mathbf{x}, \hat{\mathbf{x}}}[\mathbf{x}^T \mathbf{B}^* \hat{\mathbf{x}}]
\end{aligned}$$

Now see analyze the second term in \mathcal{L} where we prove :

$$\mathbb{E}_{\mathbf{x}}[\log(\mathbb{E}_{\tilde{\mathbf{x}}}[\exp(\mathbf{x}^T \bar{\mathbf{B}} \tilde{\mathbf{x}})])] = \mathbb{E}_{\mathbf{x}}[\log(\mathbb{E}_{\tilde{\mathbf{x}}}[\exp(\mathbf{x}^T \mathbf{B}^* \tilde{\mathbf{x}})])]$$

For this we show that the random variables $\mathbf{x}^T \mathbf{B}^* \tilde{\mathbf{x}}$ and $\mathbf{x}^T \bar{\mathbf{B}} \tilde{\mathbf{x}}$ have identical distribution. We first simplify $\mathbf{x}^T \mathbf{B}^* \tilde{\mathbf{x}}$ below.

$$\begin{aligned}
& \mathbf{x}^T \bar{\mathbf{B}} \tilde{\mathbf{x}} \\
&= \mathbf{x}^T \mathbf{R} \mathbf{B}^* \mathbf{R} \tilde{\mathbf{x}} \\
&= (\mathbf{x} - \boldsymbol{\mu}_z + \boldsymbol{\mu}_z)^T \mathbf{R} \mathbf{B}^* \mathbf{R} (\tilde{\mathbf{x}} - \boldsymbol{\mu}_{\tilde{z}} + \boldsymbol{\mu}_{\tilde{z}}) \\
&= ((\mathbf{x} - \boldsymbol{\mu}_z)^T \mathbf{R} + \boldsymbol{\mu}_z^T \mathbf{R}) \mathbf{B}^* (\mathbf{R} (\tilde{\mathbf{x}} - \boldsymbol{\mu}_{\tilde{z}}) + \mathbf{R} \boldsymbol{\mu}_{\tilde{z}}) \\
&= ((\mathbf{x} - \boldsymbol{\mu}_z)^T \mathbf{R} + \boldsymbol{\mu}_z^T \mathbf{R}) \mathbf{B}^* (\mathbf{R} (\tilde{\mathbf{x}} - \boldsymbol{\mu}_{\tilde{z}}) + \boldsymbol{\mu}_{\tilde{z}})
\end{aligned}$$

where $\boldsymbol{\mu}_z^T \mathbf{R} = \boldsymbol{\mu}_z^T (\mathbf{I} - 2\mathbf{v}\mathbf{v}^T) = \boldsymbol{\mu}_z^T - 2(\boldsymbol{\mu}_z^T \mathbf{v})\mathbf{v}^T = \boldsymbol{\mu}_z^T$. Now we prove that their distributions are identical.

$$\begin{aligned}
& \Pr(\mathbf{x}^T \bar{\mathbf{B}} \tilde{\mathbf{x}} \leq c) \\
&= \Pr(((\mathbf{x} - \boldsymbol{\mu}_z)^T \mathbf{R} + \boldsymbol{\mu}_z^T) \mathbf{B}^* (\mathbf{R} (\tilde{\mathbf{x}} - \boldsymbol{\mu}_{\tilde{z}}) + \boldsymbol{\mu}_{\tilde{z}}) \leq c) \\
&= \Pr(((\mathbf{x} - \boldsymbol{\mu}_z)^T + \boldsymbol{\mu}_z^T) \mathbf{B}^* ((\tilde{\mathbf{x}} - \boldsymbol{\mu}_{\tilde{z}}) + \boldsymbol{\mu}_{\tilde{z}}) \leq c) \\
&= \Pr(\mathbf{x} \mathbf{B}^* \tilde{\mathbf{x}} \leq c)
\end{aligned}$$

We use the fact that $(\mathbf{x} - \boldsymbol{\mu}_z)^T (\mathbf{I} - 2\mathbf{v}\mathbf{v}^T)$ is identically distributed to $(\mathbf{x} - \boldsymbol{\mu}_z)$ i.e. $\mathcal{N}(0, \mathbf{I})$.

Now since $\mathbf{x}^T \mathbf{B}^* \tilde{\mathbf{x}}, \mathbf{x}^T \bar{\mathbf{B}} \tilde{\mathbf{x}}$ are identically distributed, second term in the loss are also identically distributed and have the same expectation i.e.

$$\mathbb{E}_{\mathbf{x}}[\log(\mathbb{E}_{\tilde{\mathbf{x}}}[\exp(\mathbf{x}^T \mathbf{B}^* \tilde{\mathbf{x}})])] = \mathbb{E}_{\mathbf{x}}[\log(\mathbb{E}_{\tilde{\mathbf{x}}}[\exp(\mathbf{x}^T \bar{\mathbf{B}} \tilde{\mathbf{x}})])]$$

This proves that \mathcal{L} is identical for \mathbf{B}^* and \mathbf{B}' . But since our loss is strictly convex we have $\mathcal{L}(\frac{\mathbf{B}^* + \bar{\mathbf{B}}}{2}) < \frac{1}{2}(\mathcal{L}(\mathbf{B}^*) + \mathcal{L}(\bar{\mathbf{B}})) = \mathcal{L}(\mathbf{B}^*)$. This contradicts the fact that \mathbf{B}^* is optimal in \mathbb{S}_+^d . Hence proved. \square

B.2 Column space of A is equal to Fischer Subspace

We prove that : $\text{Col}(\mathbf{A}^*) = S_F$ when $\delta = 1$

Proof. Consider the eigendecomposition for the optimal solution \mathbf{B}^* (Eq 7). Suppose there is a direction $\mathbf{v} \in \text{Span}(\{\boldsymbol{\mu}_k\}_k)$ which is not in $\text{Span}(\{\mathbf{u}_i\}_{i \in \mathcal{I}})$.

Without loss of generality assume $\mathbf{v}^T \mathbf{u}_i = 0 \ \forall i \in \mathcal{I}$ (if not then project onto the null space and re-normalize). Now since $\lambda_j = 0 \ \forall i \notin \mathcal{I}$, we can rotate the eigenvectors $[\mathbf{u}_j]_{j \notin \mathcal{I}}$ with a unitary matrix such that $\mathbf{u}_j = v$ for some j . This operation doesn't change \mathbf{B}^*

That implies there exists \mathbf{u}_j such that $\mathbf{u}_j \in \text{Span}(\{\boldsymbol{\mu}_k\}_k)$ and $\lambda_j = 0$. We now show that

$$\frac{\partial \mathcal{L}}{\partial \lambda_j} \Big|_{\mathbf{B}=\mathbf{B}^*} < 0$$

Hence $\lambda_j > 0$ for optimal \mathbf{B}^* .

First consider the derivative of first term of \mathcal{L} with λ_j

$$\begin{aligned} \frac{\partial \mathbb{E}_{\mathbf{x}, \hat{\mathbf{x}}}[\mathbf{x}^T \mathbf{B} \hat{\mathbf{x}}]}{\partial \lambda_j} &= \left\langle \sum_k w_k \boldsymbol{\mu}_k \boldsymbol{\mu}_k^T, \frac{\partial \mathbf{B}}{\partial \lambda_j} \right\rangle \\ &= \left\langle \sum_k w_k \boldsymbol{\mu}_k \boldsymbol{\mu}_k^T, \mathbf{u}_j \mathbf{u}_j^T \right\rangle = \sum_k w_k (\boldsymbol{\mu}_k^T \mathbf{u}_j)^2 = \sum_k w_k a_k^2 \end{aligned}$$

where $a_k = \boldsymbol{\mu}_k^T \mathbf{u}_j$. Since $\mathbf{u}_j \in \text{Span}(\{\boldsymbol{\mu}_k\}_k)$ that implies there exists a non-zero a_k . Hence we have that $\frac{\partial \mathbb{E}_{\mathbf{x}, \hat{\mathbf{x}}}[\mathbf{x}^T \mathbf{B} \hat{\mathbf{x}}]}{\partial \lambda_j} > 0$ for any $\mathbf{B} \neq 0$.

For the second term in the loss we have :

$$\begin{aligned}
& \frac{\partial \mathbb{E}_{\mathbf{x}}[\log(\mathbb{E}_{\tilde{\mathbf{x}}}[\exp(\mathbf{x}^T \mathbf{B} \tilde{\mathbf{x}})])]}{\partial \lambda_j} \\
&= \mathbb{E}_{\mathbf{x}} \left[\frac{\mathbb{E}_{\tilde{\mathbf{x}}}[\exp(\mathbf{x}^T \mathbf{B} \tilde{\mathbf{x}}) \frac{\partial \mathbf{x}^T \mathbf{B} \tilde{\mathbf{x}}}{\partial \lambda_j}]}{\mathbb{E}_{\tilde{\mathbf{x}}}[\exp(\mathbf{x}^T \mathbf{B} \tilde{\mathbf{x}})]} \right] \\
&= \mathbb{E}_{\mathbf{x}} \left[\frac{\mathbb{E}_{\tilde{\mathbf{x}}}[\exp(\mathbf{x}^T \mathbf{B} \tilde{\mathbf{x}}) (\mathbf{x}^T \mathbf{u}_j) (\tilde{\mathbf{x}}^T \mathbf{u}_j)]}{\mathbb{E}_{\tilde{\mathbf{x}}}[\exp(\mathbf{x}^T \mathbf{B} \tilde{\mathbf{x}})]} \right] \\
&= \mathbb{E}_{\mathbf{x}} \left[(\mathbf{x}^T \mathbf{u}_j) \frac{\mathbb{E}_{\tilde{\mathbf{x}}}[\exp(\mathbf{x}^T \mathbf{B} \tilde{\mathbf{x}}) (\tilde{\mathbf{x}}^T \mathbf{u}_j)]}{\mathbb{E}_{\tilde{\mathbf{x}}}[\exp(\mathbf{x}^T \mathbf{B} \tilde{\mathbf{x}})]} \right] \\
&= \mathbb{E}_{\mathbf{x}} \left[(\mathbf{x}^T \mathbf{u}_j) \mathbb{E}_{\tilde{\mathbf{x}}} \left[\frac{\exp(\mathbf{x}^T \mathbf{B} \tilde{\mathbf{x}})}{\mathbb{E}_{\tilde{\mathbf{x}}}[\exp(\mathbf{x}^T \mathbf{B} \tilde{\mathbf{x}})]} \tilde{\mathbf{x}}^T \mathbf{u}_j \right] \right] \\
&= \mathbb{E}_{\mathbf{x}} \left[(\mathbf{x}^T \mathbf{u}_j) \mathbb{E}_{\tilde{\mathbf{x}}} \left[g(\tilde{\mathbf{x}}; \mathbf{x}, \mathbf{B}) \tilde{\mathbf{x}}^T \mathbf{u}_j \right] \right]
\end{aligned}$$

where we define $g(\tilde{\mathbf{x}}; \mathbf{x}, \mathbf{B})$ as :

$$g(\tilde{\mathbf{x}}; \mathbf{x}, \mathbf{B}) \triangleq \frac{\exp(\mathbf{x}^T \mathbf{B} \tilde{\mathbf{x}})}{\mathbb{E}_{\tilde{\mathbf{x}}}[\exp(\mathbf{x}^T \mathbf{B} \tilde{\mathbf{x}})]}$$

with $\mathbb{E}_{\tilde{\mathbf{x}}}[\exp(\mathbf{x}^T \mathbf{B} \tilde{\mathbf{x}})] = 1$. Also define $\mathbf{x}_{\perp} = \mathbf{u}_j (\mathbf{u}_j^T \mathbf{x})$ and $\mathbf{x}_{\parallel} = (I - \mathbf{u}_j \mathbf{u}_j^T) \mathbf{x}$. Hence $\mathbf{x} = \mathbf{x}_{\perp} + \mathbf{x}_{\parallel}$. Notice that since $\lambda_j = 0$ for \mathbf{B}^* , we have

$$g(\tilde{\mathbf{x}}; \mathbf{x}, \mathbf{B}^*) = g(\tilde{\mathbf{x}}_{\parallel}; \mathbf{x}, \mathbf{B}^*) = g(\tilde{\mathbf{x}}_{\parallel}; \mathbf{x}_{\parallel}, \mathbf{B}^*)$$

We evaluate the inner term in the above expression at $\mathbf{B} = \mathbf{B}^*$:

$$\begin{aligned}
& \mathbb{E}_{\tilde{\mathbf{x}}} \left[g(\tilde{\mathbf{x}}; \mathbf{x}, \mathbf{B}^*) \tilde{\mathbf{x}}^T \mathbf{u}_j \right] \\
&= \sum_k w_k \mathbb{E}_{\tilde{\mathbf{x}} \sim \mathcal{N}(\mu_k, I)} \left[g(\tilde{\mathbf{x}}; \mathbf{x}, \mathbf{B}^*) \tilde{\mathbf{x}}^T \mathbf{u}_j \right] \\
&= \sum_k w_k \mathbb{E}_{\tilde{\mathbf{x}} \sim \mathcal{N}(\mu_k, I)} \left[g(\tilde{\mathbf{x}}; \mathbf{x}, \mathbf{B}^*) \tilde{\mathbf{x}}^T \mathbf{u}_j \right]
\end{aligned}$$

We look at each of the expectations individually

$$\begin{aligned}
& \mathbb{E}_{\tilde{\mathbf{x}} \sim \mathcal{N}(\mu_k, I)} \left[g(\tilde{\mathbf{x}}; \mathbf{x}, \mathbf{B}^*) \tilde{\mathbf{x}}^T \mathbf{u}_j \right] \\
&= \mathbb{E}_{\tilde{\mathbf{x}} \sim \mathcal{N}(\mu_k, I)} \left[g(\tilde{\mathbf{x}}; \mathbf{x}, \mathbf{B}^*) (a_k + \tilde{\mathbf{z}}^T \mathbf{u}_j) \right] \\
&= \mathbb{E}_{\tilde{\mathbf{x}} \sim \mathcal{N}(\mu_k, I)} \left[g(\tilde{\mathbf{x}}; \mathbf{x}, \mathbf{B}^*) a_k \right] + \\
& \quad \mathbb{E}_{\tilde{\mathbf{x}} \sim \mathcal{N}(\mu_k, I)} \left[g(\tilde{\mathbf{x}}; \mathbf{x}, \mathbf{B}^*) (\tilde{\mathbf{z}}^T \mathbf{u}_j) \right] \\
&= a_k \mathbb{E}_{\tilde{\mathbf{x}} \sim \mathcal{N}(\mu_k, I)} \left[g(\tilde{\mathbf{x}}; \mathbf{x}, \mathbf{B}^*) \right] = a_k h_k(\mathbf{x}; \mathbf{B}^*)
\end{aligned}$$

where $\tilde{\mathbf{z}}$ is the noise in $\tilde{\mathbf{x}}$ and $h_k(\mathbf{x}; \mathbf{B}^*) = \mathbb{E}_{\tilde{\mathbf{x}} \sim \mathcal{N}(\mu_k, I)} \left[g(\tilde{\mathbf{x}}; \mathbf{x}, \mathbf{B}^*) \right]$. We use the property that $\tilde{\mathbf{z}}_\perp$ is independent of $g(\tilde{\mathbf{x}}; \mathbf{x}, \mathbf{B}^*) = g(\tilde{\mathbf{x}}_\parallel; \mathbf{x}, \mathbf{B}^*)$ to show that its equal to 0.

$$\begin{aligned} & \mathbb{E}_{\tilde{\mathbf{x}} \sim \mathcal{N}(\mu_k, I)} \left[g(\tilde{\mathbf{x}}_\parallel; \mathbf{x}, \mathbf{B}^*) (\tilde{\mathbf{z}}_\perp^T \mathbf{u}_j) \right] \\ &= \mathbb{E}_{\tilde{\mathbf{x}} \sim \mathcal{N}(\mu_k, I)} \left[g(\tilde{\mathbf{x}}_\parallel; \mathbf{x}, \mathbf{B}^*) \right] \mathbb{E}_{\tilde{\mathbf{x}} \sim \mathcal{N}(\mu_k, I)} \left[\tilde{\mathbf{z}}_\perp^T \mathbf{u}_j \right] \\ &= \mathbb{E}_{\tilde{\mathbf{x}} \sim \mathcal{N}(\mu_k, I)} \left[g(\tilde{\mathbf{x}}_\parallel; \mathbf{x}, \mathbf{B}^*) \right] * 0 = 0 \end{aligned}$$

Hence we have

$$\mathbb{E}_{\tilde{\mathbf{x}}} \left[g(\tilde{\mathbf{x}}; \mathbf{x}, \mathbf{B}^*) \tilde{\mathbf{x}}^T \mathbf{u}_j \right] = \sum_k w_k a_k h_k(\mathbf{x}; \mathbf{B}^*)$$

We have $\sum_k w_k h_k(\mathbf{x}) = 1$

$$\begin{aligned} & \sum_k w_k h_k(\mathbf{x}; \mathbf{B}) \\ &= \sum_k w_k \mathbb{E}_{\tilde{\mathbf{x}} \sim \mathcal{N}(\mu_k, I)} \left[g(\tilde{\mathbf{x}}_\parallel; \mathbf{x}, \mathbf{B}) \right] \\ &= \sum_k w_k \mathbb{E}_{\tilde{\mathbf{x}} \sim \mathcal{N}(\mu_k, I)} \left[\frac{\exp(\mathbf{x}^T \mathbf{B} \tilde{\mathbf{x}})}{\mathbb{E}_{\tilde{\mathbf{x}}} [\exp(\mathbf{x}^T \mathbf{B} \tilde{\mathbf{x}})]} \right] \\ &= \mathbb{E}_{\tilde{\mathbf{x}}} \left[\frac{\exp(\mathbf{x}^T \mathbf{B} \tilde{\mathbf{x}})}{\mathbb{E}_{\tilde{\mathbf{x}}} [\exp(\mathbf{x}^T \mathbf{B} \tilde{\mathbf{x}})]} \right] = 1 \end{aligned}$$

While $g(\tilde{\mathbf{x}}; \mathbf{x}, \mathbf{B})$, is the weight \mathbf{x} gives to a point $\tilde{\mathbf{x}}$, $h_k(\mathbf{x}; \mathbf{B})$ can be interpreted as a weight \mathbf{x} gives to cluster k (i.e. expectation of g over a cluster).

Going back to the expression at $\mathbf{B} = \mathbf{B}^*$

$$\begin{aligned} & \mathbb{E}_{\mathbf{x}} \left[(\mathbf{x}^T \mathbf{u}_j) \mathbb{E}_{\tilde{\mathbf{x}}} \left[g(\tilde{\mathbf{x}}; \mathbf{x}, \mathbf{B}^*) \tilde{\mathbf{x}}^T \mathbf{u}_j \right] \right] \\ &= \mathbb{E}_{\mathbf{x}} \left[(\mathbf{x}^T \mathbf{u}_j) \sum_k w_k a_k h_k(\mathbf{x}; \mathbf{B}^*) \right] \\ &= \sum_k w_k a_k \mathbb{E}_{\mathbf{x}} \left[(\mathbf{x}^T \mathbf{u}_j) h_k(\mathbf{x}; \mathbf{B}^*) \right] \\ &= \sum_k w_k a_k \mathbb{E}_{\mathbf{x}} \left[(\mathbf{x}^T \mathbf{u}_j) h_k(\mathbf{x}; \mathbf{B}^*) \right] \\ &= \sum_k w_k a_k \sum_{k'} w_{k'} \mathbb{E}_{\mathbf{x} \sim \mathcal{N}(\mu_{k'}, I)} \left[(\mathbf{x}^T \mathbf{u}_j) h_k(\mathbf{x}; \mathbf{B}^*) \right] \end{aligned}$$

h inherits the property $h_k(\mathbf{x}; \mathbf{B}^*) = h_k(\mathbf{x}_{\parallel}; \mathbf{B}^*)$ from g (this is because $\lambda_j = 0$ in \mathbf{B}^*). Evaluating the inner expression we have

$$\begin{aligned}
& \mathbb{E}_{\mathbf{x} \sim \mathcal{N}(\boldsymbol{\mu}_{k'}, I)} \left[(\mathbf{x}^T \mathbf{u}_j) h_k(\mathbf{x}; \mathbf{B}^*) \right] \\
&= \mathbb{E}_{\mathbf{x} \sim \mathcal{N}(\boldsymbol{\mu}_{k'}, I)} \left[(a_{k'} + \mathbf{z}_{\perp}^T \mathbf{u}_j) h_k(\mathbf{x}; \mathbf{B}^*) \right] \\
&= a_{k'} \mathbb{E}_{\mathbf{x} \sim \mathcal{N}(\boldsymbol{\mu}_{k'}, I)} \left[h_k(\mathbf{x}; \mathbf{B}^*) \right] \\
&\quad + \mathbb{E}_{\mathbf{x} \sim \mathcal{N}(\boldsymbol{\mu}_{k'}, I)} \left[(\mathbf{z}_{\perp}^T \mathbf{u}_j) h_k(\mathbf{x}; \mathbf{B}^*) \right] \\
&= a_{k'} \mathbb{E}_{\mathbf{x} \sim \mathcal{N}(\boldsymbol{\mu}_{k'}, I)} \left[h_k(\mathbf{x}; \mathbf{B}^*) \right] = a_{k'} f_{k', k}
\end{aligned}$$

where \mathbf{z} is the noise in \mathbf{x} . We use the property that \mathbf{z}_{\perp} is independent of $h_k(\mathbf{x}; \mathbf{B}^*) = h_k(\mathbf{x}_{\parallel}; \mathbf{B}^*)$ to show that its equal to 0.

$$\begin{aligned}
\sum_k w_k f_{k', k} &= \sum_k w_k \mathbb{E}_{\mathbf{x} \sim \mathcal{N}(\boldsymbol{\mu}_{k'}, I)} \left[h_k(\mathbf{x}; \mathbf{B}^*) \right] \\
&\quad \mathbb{E}_{\mathbf{x} \sim \mathcal{N}(\boldsymbol{\mu}_{k'}, I)} \left[\sum_k w_k h_k(\mathbf{x}; \mathbf{B}^*) \right] = 1
\end{aligned}$$

since $\sum_k w_k h_k(\mathbf{x}; \mathbf{B}^*) = 1$.

Define a matrix $\mathbf{F} \in \mathbb{R}^{K \times K}$ as $\mathbf{F}_{i,j} = f_{i,j}$ and $\mathbf{W} = \text{diag}(w_1, w_2, \dots, w_K)$ and $\mathbf{a} = [a_1, a_2, \dots, a_K]^T$.

$$\begin{aligned}
& \mathbb{E}_{\mathbf{x}} \left[(\mathbf{x}^T \mathbf{u}_j) \mathbb{E}_{\tilde{\mathbf{x}}} \left[g(\tilde{\mathbf{x}}; \mathbf{x}, \mathbf{B}^*) \tilde{\mathbf{x}}^T \mathbf{u}_j \right] \right] \\
&= \sum_k w_k a_k \sum_{k'} w_{k'} \mathbb{E}_{\mathbf{x} \sim \mathcal{N}(\boldsymbol{\mu}_{k'}, I)} \left[(\mathbf{x}^T \mathbf{u}_j) h_k(\mathbf{x}; \mathbf{B}^*) \right] \\
&= \sum_k w_k a_k \sum_{k'} w_{k'} a_{k'} f_{k', k} \\
&= \mathbf{a}^T \mathbf{W} \mathbf{F} \mathbf{W} \mathbf{a} = (\sqrt{\mathbf{W}} \mathbf{a})^T \sqrt{\mathbf{W}} \mathbf{F} \sqrt{\mathbf{W}} (\sqrt{\mathbf{W}} \mathbf{a})
\end{aligned}$$

Eigenvalues of $\sqrt{\mathbf{W}} \mathbf{F} \sqrt{\mathbf{W}}$ are equal to eigenvalues of $\mathbf{F} \mathbf{W}$ (since this is a similarity transform). And if \mathbf{v} is eigenvector of $\mathbf{F} \mathbf{W}$, then $\sqrt{\mathbf{W}} \mathbf{v}$ is the eigenvector for $\sqrt{\mathbf{W}} \mathbf{F} \sqrt{\mathbf{W}}$.

Since \mathbf{F} has expectation of exponentials as its entries i.e. $\mathbf{F}_{i,j} > 0$ and $\mathbf{W} > 0$ from definition. Hence we have that every entry of $\mathbf{F} \mathbf{W}$ is strictly greater than 0. The Perron–Frobenius eigenvalue r is given by

$$\min_i \sum_j (\mathbf{F} \mathbf{W})_{i,j} \leq r \leq \max_i \sum_j (\mathbf{F} \mathbf{W})_{i,j}$$

But we have that for every i the sum is equal to 1.

$$\sum_j (\mathbf{F}\mathbf{W})_{i,j} = \sum_j \sum_l (\mathbf{F}_{i,l} \mathbf{W}_{l,j}) = \sum_j f_{i,j} w_j = 1$$

Hence $r = 1$ and the Perron vector is simply $\mathbf{1} = [1, 1, \dots, 1] \in \mathbb{R}^K$. Hence we show that eigenvector with largest eigenvalue (i.e. 1) for $\sqrt{\mathbf{W}}\mathbf{F}\sqrt{\mathbf{W}}$ is $\sqrt{\mathbf{W}}\mathbf{1}$. Hence we have that

$$(\sqrt{\mathbf{W}}\mathbf{a})^T \sqrt{\mathbf{W}}\mathbf{F}\sqrt{\mathbf{W}}(\sqrt{\mathbf{W}}\mathbf{a}) \leq \|\sqrt{\mathbf{W}}\mathbf{a}\|^2 = \sum_k w_k a_k^2$$

The equality only holds when $\mathbf{a} \in \text{Span}(\mathbf{1})$, i.e. all a_k are equal. This is not true (since $\sum_k a_k = 0$ and there exists a nonzero a_k). Hence

$$\mathbb{E}_{\mathbf{x}} \left[(\mathbf{x}^T \mathbf{u}_j) \mathbb{E}_{\tilde{\mathbf{x}}} \left[g(\tilde{\mathbf{x}}; \mathbf{x}, \mathbf{B}^*) \tilde{\mathbf{x}}^T \mathbf{u}_j \right] \right] < \sum_k w_k a_k^2$$

The loss for the whole term is

$$\begin{aligned} \frac{\partial \mathcal{L}}{\partial \lambda_j} \Big|_{\mathbf{B}=\mathbf{B}^*} &= - \frac{\partial \mathbb{E}_{\mathbf{x}, \hat{\mathbf{x}}} [\mathbf{x}^T \mathbf{B} \hat{\mathbf{x}}]}{\partial \lambda_j} \\ &\quad + \frac{\partial \mathbb{E}_{\mathbf{x}} [\log(\mathbb{E}_{\tilde{\mathbf{x}}} [\exp(\mathbf{x}^T \mathbf{B} \tilde{\mathbf{x}})])]}{\partial \lambda_j} \\ &< - \sum_k w_k a_k^2 + \sum_k w_k a_k^2 = 0 \end{aligned}$$

Hence proved. □

C Proof for InfoNCE loss

In this section, we use Prop B.1 to prove our main theorem. We recommend the reader to first go through Prop B.1 and its proof (in Suppl B) to understand the proof for the main theorem.

Proof.

$$\mathcal{L} = -\mathbb{E}_{\mathbf{x}, \hat{\mathbf{x}}} [\mathbf{x}^T \mathbf{B} \hat{\mathbf{x}}] + \mathbb{E}_{\mathbf{x}} [\log(\mathbb{E}_{\tilde{\mathbf{x}}} [\exp(\mathbf{x}^T \mathbf{B} \tilde{\mathbf{x}})])]$$

where $\mathbf{B} = \mathbf{A}\mathbf{A}^T$, i.e. \mathbf{B} is positive semi-definite (PSD) matrix of rank r . The above step follows from Proposition B.1. We relax the rank-constraint on \mathbf{B} . We finally show that rank of \mathbf{B}^* i.e. the optimal solution $\leq K$ which satisfies the above condition as $K \leq r$.

Now consider a change of variables given by $\mathbf{x}' = \Sigma^{-\frac{1}{2}}\mathbf{x}$. This implies that \mathbf{x}' now follows a GMM with means given by $\{\Sigma^{-\frac{1}{2}}\boldsymbol{\mu}_k\}_{k \in [K]}$ and isotropic covariance \mathbf{I} (as $\mathbb{E}[\mathbf{x}'\mathbf{x}'^T] = \mathbb{E}[\Sigma^{-\frac{1}{2}}\mathbf{x}\mathbf{x}^T\Sigma^{-\frac{1}{2}}] = \Sigma^{-\frac{1}{2}}\mathbb{E}[\mathbf{x}\mathbf{x}^T]\Sigma^{-\frac{1}{2}} = \mathbf{I}$).

The loss be hence be written as :

$$\begin{aligned}\mathcal{L} = & -\mathbb{E}_{\mathbf{x}', \hat{\mathbf{x}}'}[\mathbf{x}'^T \boldsymbol{\Sigma}^{\frac{1}{2}} \mathbf{B} \boldsymbol{\Sigma}^{\frac{1}{2}} \hat{\mathbf{x}}'] \\ & + \mathbb{E}_{\mathbf{x}'}[\log(\mathbb{E}_{\tilde{\mathbf{x}}'}[\exp(\mathbf{x}'^T \boldsymbol{\Sigma}^{\frac{1}{2}} \mathbf{B} \boldsymbol{\Sigma}^{\frac{1}{2}} \tilde{\mathbf{x}}')])]\end{aligned}$$

Now let $\mathbf{B}' = \boldsymbol{\Sigma}^{\frac{1}{2}} \mathbf{B} \boldsymbol{\Sigma}^{\frac{1}{2}}$. \mathbf{B}' is also a PSD matrix. Hence loss can be written as :

$$\mathcal{L} = -\mathbb{E}_{\mathbf{x}', \hat{\mathbf{x}}'}[\mathbf{x}'^T \mathbf{B}' \hat{\mathbf{x}}'] + \mathbb{E}_{\mathbf{x}'}[\log(\mathbb{E}_{\tilde{\mathbf{x}}'}[\exp(\mathbf{x}'^T \mathbf{B}' \tilde{\mathbf{x}}')])]$$

Let the optimal \mathbf{B}'^* be denoted by $\sum_i \lambda_i \mathbf{u}_i \mathbf{u}_i^T$ and let \mathcal{I} be set of indices with $\lambda_i > 0$ (note $\lambda_i \geq 0 \forall i$). But from Proposition B.1, we know that , where $\text{Span}\{\mathbf{u}_i\}_{i \in \mathcal{I}} = \text{Span}\{\boldsymbol{\mu}'_k\}_{k \in [K]}$ where $\{\boldsymbol{\mu}'_k\}$ is the set of means.

For an invertible $\boldsymbol{\Sigma}$ and $\boldsymbol{\mu}'_k = \boldsymbol{\Sigma}^{-\frac{1}{2}} \boldsymbol{\mu}_k$, we have

$$\begin{aligned}\text{Span}\{\mathbf{u}_i\}_{i \in \mathcal{I}} &= \text{Span}\{\boldsymbol{\mu}'_k\} \\ \implies \text{Span}\{\mathbf{u}_i\}_{i \in \mathcal{I}} &= \text{Span}\{\boldsymbol{\Sigma}^{-\frac{1}{2}} \boldsymbol{\mu}_k\} \\ \implies \text{Span}\{\boldsymbol{\Sigma}^{-\frac{1}{2}} \mathbf{u}_i\}_{i \in \mathcal{I}} &= \text{Span}\{\boldsymbol{\Sigma}^{-1} \boldsymbol{\mu}_k\}\end{aligned}$$

Substituting and $\mathbf{B}^* = \boldsymbol{\Sigma}^{-\frac{1}{2}} \mathbf{B}'^* \boldsymbol{\Sigma}^{-\frac{1}{2}}$ we get :

$$\begin{aligned}\mathbf{B}^* &= \boldsymbol{\Sigma}^{-\frac{1}{2}} \left(\sum_i \lambda_i \mathbf{u}_i \mathbf{u}_i^T \right) \boldsymbol{\Sigma}^{-\frac{1}{2}} \\ &= \sum_i (\sqrt{\lambda_i} \boldsymbol{\Sigma}^{-\frac{1}{2}} \mathbf{u}_i) (\sqrt{\lambda_i} \boldsymbol{\Sigma}^{-\frac{1}{2}} \mathbf{u}_i)^T\end{aligned}$$

Hence the optimal solution in the original space $\mathbf{A}^* = \left[\sqrt{\lambda_i} \boldsymbol{\Sigma}^{-\frac{1}{2}} \mathbf{u}_i \right]_{i \in \mathcal{I}}$. We proved that $\text{Span}\{\boldsymbol{\Sigma}^{-\frac{1}{2}} \mathbf{u}_i\}_{i \in \mathcal{I}} = \text{Span}\{\boldsymbol{\Sigma}^{-1} \boldsymbol{\mu}_k\}_{k \in [K]}$. This implies that column space of $\text{Col}(\mathbf{A}^*) = \text{Span}\{\boldsymbol{\Sigma}^{-\frac{1}{2}} \mathbf{u}_i\}_{i \in \mathcal{I}} = \text{Span}\{\boldsymbol{\Sigma}^{-1} \boldsymbol{\mu}_k\}_{k \in [K]}$. Hence proved.

□

D Proof for SimSiam Loss

In this section, we use the same methodology as in part of Prop B.1 to prove the theorem. First we use the strict convexity of the loss to show that the solution lies in the fisher subspace. Afterwards, by differentiating the loss function w.r.t. any direction in the fisher subspace, we show that all directions in the subspace should be learnt assuming sufficient capacity.

Proof. We write the objective by computing the expectations as :

$$\begin{aligned}
\mathcal{L}_{SS}(\mathbf{A}) &= -\mathbb{E}_{(\mathbf{x}, \hat{\mathbf{x}}) \sim \hat{F}} \left[(\mathbf{A}^T \mathbf{x})^T \mathbf{A}^T \hat{\mathbf{x}} \right] + \xi \mathbb{E}_{\mathbf{x} \sim F} \left[\|\mathbf{A}^T \mathbf{x}\|^2 \right] \\
&= -\mathbb{E}_{(\mathbf{x}, \hat{\mathbf{x}}) \sim \hat{F}} \left[\langle \mathbf{A} \mathbf{A}^T, \hat{\mathbf{x}} \mathbf{x}^T \rangle \right] + \xi \mathbb{E}_{\mathbf{x} \sim F} \left[\langle \mathbf{A} \mathbf{A}^T, \mathbf{x} \mathbf{x}^T \rangle \right] \\
&= -\langle \mathbf{A} \mathbf{A}^T, \mathbb{E}_{(\mathbf{x}, \hat{\mathbf{x}}) \sim \hat{F}} [\hat{\mathbf{x}} \mathbf{x}^T] \rangle + \xi \langle \mathbf{A} \mathbf{A}^T, \mathbb{E}_{\mathbf{x} \sim F} [\mathbf{x} \mathbf{x}^T] \rangle \\
&= -\langle \mathbf{A} \mathbf{A}^T, \sum_k w_k \boldsymbol{\mu}_k \boldsymbol{\mu}_k^T \rangle + \xi \langle \mathbf{A} \mathbf{A}^T, \sum_k w_k \boldsymbol{\mu}_k \boldsymbol{\mu}_k^T + \boldsymbol{\Sigma} \rangle \\
&= \langle \mathbf{B}, (-\delta + \xi) \mathbf{M} \rangle + \xi \langle \mathbf{B}, \boldsymbol{\Sigma} \rangle \\
&= \langle \mathbf{B}, (-\delta + \xi) \mathbf{M} + \xi \boldsymbol{\Sigma} \rangle \\
&= \langle \boldsymbol{\Sigma}^{\frac{1}{2}} \mathbf{B} \boldsymbol{\Sigma}^{\frac{1}{2}}, (-\delta + \xi) \boldsymbol{\Sigma}^{-\frac{1}{2}} \mathbf{M} \boldsymbol{\Sigma}^{-\frac{1}{2}} + \xi \mathbf{I} \rangle \\
&= \langle \mathbf{B}', (-\delta + \xi) \mathbf{M}' + \xi \mathbf{I} \rangle
\end{aligned}$$

where we have $\mathbf{B} = \mathbf{A} \mathbf{A}^T$, $\mathbf{M} = \sum_k w_k \boldsymbol{\mu}_k \boldsymbol{\mu}_k^T$, $\mathbf{B}' = \boldsymbol{\Sigma}^{\frac{1}{2}} \mathbf{B} \boldsymbol{\Sigma}^{\frac{1}{2}}$ and $\mathbf{M}' = \boldsymbol{\Sigma}^{-\frac{1}{2}} \mathbf{M} \boldsymbol{\Sigma}^{-\frac{1}{2}}$. Note that the loss is linear in \mathbf{B} (and \mathbf{B}'). Since we restrict ourselves to $\|\mathbf{A}\|_2 \leq 1$, it is also true that $\|\mathbf{B}\|_2 \leq 1$.

We now show that the optimal \mathbf{B}' has column space (and row space, since symmetric) lying in column space (and row space) of \mathbf{M}' . Let \mathbf{B}^* be the optimal solution. Denote the eigendecomposition of \mathbf{B}^* as $\mathbf{U} \boldsymbol{\Lambda} \mathbf{U}^T$, where $\boldsymbol{\Lambda} \succeq 0$ (as $\mathbf{B} \succeq 0$) and \mathbf{U} is a unitary matrix. Equivalently :

$$\mathbf{B}^* = \sum_i \lambda_i \mathbf{u}_i \mathbf{u}_i^T \quad (7)$$

where \mathbf{u}_i are columns of \mathbf{U} . Suppose the condition is not true. Then there exists a unit vector \mathbf{v} , such that $\mathbf{M}' \mathbf{v} = 0$ and $\mathbf{B}' \mathbf{v} \neq 0$.

We construct a new matrix $\bar{\mathbf{U}}$, whose columns are projection of \mathbf{U} onto the plane with normal vector \mathbf{v} given by $\mathbf{R} = \mathbf{I} - \mathbf{v} \mathbf{v}^T$. The projection matrix is defined such that $\mathbf{R} \mathbf{M}' = \mathbf{M}'$. Define $\bar{\mathbf{B}}$ from the constructed $\bar{\mathbf{U}}$.

$$\begin{aligned}
\bar{\mathbf{U}} &= \mathbf{R} \mathbf{U} = (\mathbf{I} - \mathbf{v} \mathbf{v}^T) \mathbf{U} \\
\bar{\mathbf{B}} &= \bar{\mathbf{U}} \boldsymbol{\Lambda} \bar{\mathbf{U}}^T = \mathbf{R} \mathbf{B}^* \mathbf{R}^T
\end{aligned}$$

Now through some algebra we see that loss at $\bar{\mathbf{B}}$ is less than at \mathbf{B}^* and hence \mathbf{B}^* can't be optimal.

$$\begin{aligned}
&\langle \bar{\mathbf{B}}, (-\delta + \xi) \mathbf{M}' + \xi \mathbf{I} \rangle \\
&= \langle \mathbf{B}^*, (-\delta + \xi) \mathbf{R}^T \mathbf{M}' \mathbf{R} + \xi \mathbf{R}^T \mathbf{R} \rangle \\
&= \langle \mathbf{B}^*, (-\delta + \xi) \mathbf{M}' + \xi \mathbf{I} + \xi (\mathbf{R}^T \mathbf{R} - \mathbf{I}) \rangle \\
&= \langle \mathbf{B}^*, (-\delta + \xi) \mathbf{M}' + \xi \mathbf{I} \rangle + \xi \langle \mathbf{B}^*, (\mathbf{R}^T \mathbf{R} - \mathbf{I}) \rangle
\end{aligned}$$

Now we show that $\langle \mathbf{B}^*, (\mathbf{R}^T \mathbf{R} - \mathbf{I}) \rangle < 0$ and since $\xi > 0$, loss at $\bar{\mathbf{B}}$ is less than at \mathbf{B}^* . The fact is intuitively clear and a formal proof is as follows :

$$\langle \mathbf{B}^*, \mathbf{R}^T \mathbf{R} \rangle = \text{tr}(\mathbf{R} \mathbf{B}^* \mathbf{R}^T) = \sum_i \lambda_i \|\mathbf{R} \mathbf{u}_i\|_2^2 < \sum_i \lambda_i \|\mathbf{u}_i\|_2^2 = \langle \mathbf{B}^*, \mathbf{I} \rangle$$

The strict inequality is due to fact that $\mathbf{B}' \mathbf{v} \neq 0$, i.e. there exists a i with $\lambda_i > 0$ and $\mathbf{v}^T \mathbf{u}_i \neq 0$ (and hence $\|\mathbf{R} \mathbf{u}_i\|_2^2 < \|\mathbf{u}_i\|_2^2$). $\|\mathbf{R} \mathbf{u}_j\|_2^2 \leq \|\mathbf{u}_j\|_2^2$ is true generally because \mathbf{R} is a projection matrix.

Hence we showed that column space of \mathbf{B}^* (i.e., optimal \mathbf{B}') lies in column space of \mathbf{M}' . Now we show that it **spans the whole column space**. Suppose not. Let \mathbf{B}^* be the optimal solution with decomposition with notation as used above. Then WLOG there exists \mathbf{u}_i which $\in \text{Span}(\mathbf{M}')$ and $\lambda_i = 0$ (if it doesn't exist we can rotate the \mathbf{u}_j 's with 0 eigenvalues so that a \mathbf{u}_i aligns in the subspace). We take derivative w.r.t. λ_i and show that it's negative.

$$\begin{aligned} \frac{\partial \mathcal{L}_{SS}}{\partial \lambda_i} \Big|_{\mathbf{B}'=\mathbf{B}^*} &= \frac{\partial \langle \mathbf{B}', (-\delta + \xi) \mathbf{M}' + \xi \mathbf{I} \rangle}{\partial \lambda_i} \\ &= \mathbf{u}_i^T ((-\delta + \xi) \mathbf{M}' + \xi \mathbf{I}) \mathbf{u}_i \\ &= (-\delta + \xi) \mathbf{u}_i^T \mathbf{M}' \mathbf{u}_i + \xi \end{aligned}$$

if $\xi < \frac{\delta \mathbf{v}^T \mathbf{M}' \mathbf{v}}{1 + \mathbf{v}^T \mathbf{M}' \mathbf{v}}$ for all directions \mathbf{v} in $\text{Span}(\mathbf{M}')$ (as $\mathbf{u}_i \in \text{Span}(\mathbf{M}')$), then $\frac{\partial \mathcal{L}_{SS}}{\partial \lambda_i}$ is < 0 . $\frac{\delta \mathbf{v}^T \mathbf{M}' \mathbf{v}}{1 + \mathbf{v}^T \mathbf{M}' \mathbf{v}}$ is monotonic in $\mathbf{v}^T \mathbf{M}' \mathbf{v}$. The minimum value of $\mathbf{v}^T \mathbf{M}' \mathbf{v}$ is the smallest non-zero eigenvalue of \mathbf{M}' denoted by λ_{\min} . Hence if $0 < \xi < \frac{\delta \lambda_{\min}}{1 + \lambda_{\min}}$ we are good.

Now we showed that \mathbf{B}^* (i.e., optimal \mathbf{B}') spans the complete column space of \mathbf{M}' . Hence using the facts $\mathbf{B}' = \Sigma^{\frac{1}{2}} \mathbf{B} \Sigma^{\frac{1}{2}}$ and $\mathbf{B} = \mathbf{A}^T \mathbf{A}$, we can argue that for the optimal value of \mathbf{A} denoted by \mathbf{A}^* , $\text{Col}(\mathbf{A}^*) = S_F$. \square

E Proof for CLIP Loss

In this section, we use the first part of Prop B.1 to prove the theorem, i.e. we use the proof of $\text{Col}(\mathbf{A}^*) \subseteq S_F$.

Proof. We write the objective by substituting the functional form of f as :

$$\begin{aligned} \mathcal{L} &= -\mathbb{E}_{\mathbf{x}_t, \mathbf{x}_v} [\mathbf{x}_t^T \mathbf{A}_t \mathbf{A}_v^T \mathbf{x}_v] \\ &\quad + \mathbb{E}_{\mathbf{x}_t} [\log(\mathbb{E}_{\tilde{\mathbf{x}}_v} [\exp(\mathbf{x}_t^T \mathbf{A}_t \mathbf{A}_v^T \tilde{\mathbf{x}}_v)])] \\ &= -\mathbb{E}_{\mathbf{x}_t, \mathbf{x}_v} [\mathbf{x}_t^T \mathbf{B} \mathbf{x}_v] + \mathbb{E}_{\mathbf{x}_t} [\log(\mathbb{E}_{\tilde{\mathbf{x}}_v} [\exp(\mathbf{x}_t^T \mathbf{B} \tilde{\mathbf{x}}_v)])] \end{aligned}$$

where $\mathbf{B} = \mathbf{A}_t \mathbf{A}_v^T$. We can further do a change of variable by $\mathbf{x}'_t = \Sigma_t^{-\frac{1}{2}} \mathbf{x}_t$ and $\mathbf{x}'_v = \Sigma_v^{-\frac{1}{2}} \mathbf{x}_v$. The means are now $\boldsymbol{\mu}'_{t,k} = \Sigma_t^{-\frac{1}{2}} \boldsymbol{\mu}_{t,k}$ and $\boldsymbol{\mu}'_{v,k} = \Sigma_v^{-\frac{1}{2}} \boldsymbol{\mu}_{v,k}$. Define $\mathbf{B}' = \Sigma_t^{\frac{1}{2}} \mathbf{B} \Sigma_v^{\frac{1}{2}}$. Now \mathbf{x}'_t and \mathbf{x}'_v have

components with covariance being isotropic. Now we have :

$$\begin{aligned}\mathcal{L} &= -\mathbb{E}_{\mathbf{x}_t, \mathbf{x}_v} [\mathbf{x}_t^T \mathbf{B} \mathbf{x}_v] + \mathbb{E}_{\mathbf{x}_t} [\log(\mathbb{E}_{\tilde{\mathbf{x}}_v} [\exp(\mathbf{x}_t^T \mathbf{B} \tilde{\mathbf{x}}_v)])] \\ &= -\mathbb{E}_{\mathbf{x}'_t, \mathbf{x}'_v} [\mathbf{x}'_t^T \mathbf{B}' \mathbf{x}'_v] + \mathbb{E}_{\mathbf{x}'_t} [\log(\mathbb{E}_{\tilde{\mathbf{x}}'_v} [\exp(\mathbf{x}'_t^T \mathbf{B}' \tilde{\mathbf{x}}'_v)])]\end{aligned}$$

We argue that optimal \mathbf{B}'^* has its row space equal to $\text{Span}\{\boldsymbol{\mu}'_{v,k}\}$ and its column space equal to $\text{Span}\{\boldsymbol{\mu}'_{t,k}\}$. We present the argument for column space (row space argument follows similarly).

Suppose there exists a unit vector \mathbf{v} such that $\mathbf{v}^T \boldsymbol{\mu}'_{t,k} = 0$ for all $k \in [K]$, $\mathbf{v}^T \mathbf{B}'^* \neq 0$. Then we can define a new matrix as $\bar{\mathbf{B}}' = \mathbf{R} \mathbf{B}'^* = (I - 2\mathbf{v}\mathbf{v}^T) \mathbf{B}'^*$, where $\mathbf{R} = I - 2\mathbf{v}\mathbf{v}^T$ is a reflection matrix. Following arguments from Proposition B.1 we can prove that $\mathbf{x}'_t^T \mathbf{B}'^* \tilde{\mathbf{x}}'_v$ is identically distributed to $\mathbf{x}'_t^T \bar{\mathbf{B}}' \tilde{\mathbf{x}}'_v$. Hence using this we can show that $\mathcal{L}(\mathbf{B}'^*) = \mathcal{L}(\bar{\mathbf{B}}')$. Then by the strict convexity of the loss function \mathcal{L} we have that $\mathcal{L}\left(\frac{\mathbf{B}'^* + \bar{\mathbf{B}}'}{2}\right) < \frac{\mathcal{L}(\mathbf{B}'^*) + \mathcal{L}(\bar{\mathbf{B}}')}{2} = \mathcal{L}(\mathbf{B}'^*)$. Hence \mathbf{B}'^* can't be optimal.

Hence proved. \square

F Representation collapse in non-contrastive learning

Consider a two component GMM in a d dimensional ambient space. The means of the components lie on the x and y axis (i.e. the first two dimensions), equidistant from the origin. Both components have isotropic covariance. We plot the first two dimensions in the figure below 3. Note that for this

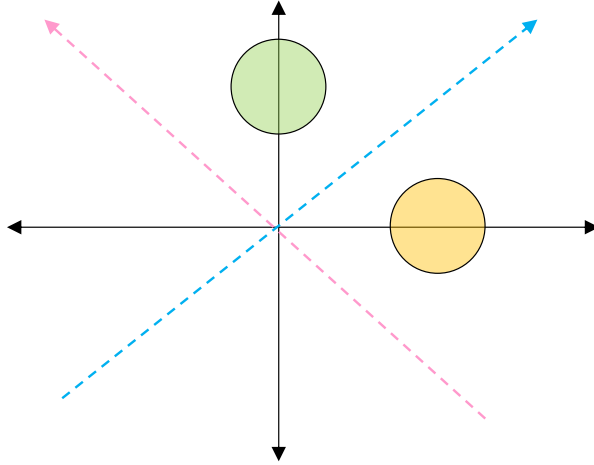


Figure 3: Caption

setup the rank of the fisher subspace is two (i.e., $K = 2$) and the fisher subspace is the $x - y$ plane.

Consider learning a mapping matrix onto a one-dimensional subspace (i.e. $r < K$). InfoNCE type contrastive objectives would learn the subspace given by the pink line (i.e. gaussian would be projected onto the pink line and hence would be well separated). This is stated without proof, but we know that InfoNCE loss would learn a subspace lying in the fisher subspace. And through some basic algebra we can convince ourselves that the solution would be the pink like (i.e. the line $x + y = 0$).

But for non-contrastive objectives like SimSiam, while we can only prove that the optimal solution lies in the $x - y$ plane. SimSiam objective is not able to distinguish between the lines $x + y = 0$ and $x = y$, and hence might lead to collapse of representations. But as stated in the theorem ??, this is

only if $r < K$. For $r \geq K$, the SimSiam objective learns the complete fisher subspace (and only the fisher subspace).

G Experimental Details

G.1 Data Generation

We also ensure that . For directions orthogonal to the mean-subspace we upscale the variance by a factor of κ . **Ambient Dimension** We consider the ambient dimension to be 100 for all experiments (except for Scaling plot Fig 2d, where we let ambient dimension equal to $K - 1$). **Means of Components** For generation means of the components, we first sample $K - 1$ times from a 0 mean, \mathbf{I} normal distribution in ambient dimension space. We chose the K th mean such that the means sum upto 0. Hence the means lie in a $K - 1 = 9$ dimensional space. **Covariance Matrix** To construct a covariance matrix we start with a unit variance \mathbf{I} matrix. We then upscale the variance in (Ambient - NumMeans+1) dimensional space orthogonal to the means subspace by factor of κ , where $\kappa = \sigma_{\max}(\boldsymbol{\Sigma})/\sigma_{\min}(\boldsymbol{\Sigma})$. We take κ to be $1/0.1 = 10.0$ by default. For scaling experiments, we choose random NumMeans/2 orthogonal directions, and increase the covariance in those directions. Note for condition number experiment we take κ to be $1/0.x$ where x goes from 1 to 9.

G.2 Orthonormalized InfoNCE and SimSiam

We plot the ARI/AMI numbers for orthonormalized InfoNCE and SimSiam matrices in Fig 4. Specifically, we do a QR decomposition on these matrices and take the orthogonal Q matrix as the projection matrix. In these plots the convergence issues of InfoNCE loss become more apparent, as we can see that InfoNCE lagging behind optimal.

H Linear Discriminant Analysis (LDA) and Fisher LDA

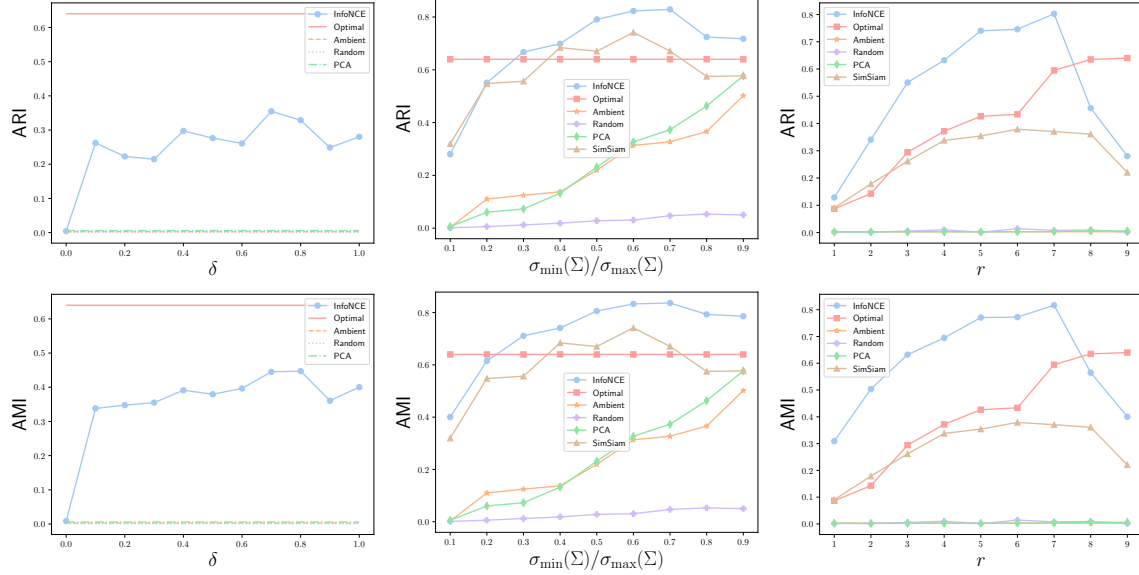
H.1 Linear Discriminant Analysis

The classical binary class LDA objective is defined as a bayes-optimal solution for classification under the assumption that the data is generated from a two-component Gaussian mixture model with identical covariances. For non-shared covariance for two component case we don't have a closed form solution and the problem is referred to as Quadratic discriminant Analysis. The LDA solution for two-component GMM with shared covariance is the subspace projection on which leads to no loss in likelihood of data. It is given as :

$$\mathcal{S}_{LDA} = \boldsymbol{\Sigma}^{-1}(\boldsymbol{\mu}_1 - \boldsymbol{\mu}_2)$$

H.2 Fischer Linear Discriminant Analysis

Instead of defining the LDA objective to be the Bayes-optimal under the assumption that data is generated from a two-component Gaussian mixture model with shared covariance, Fischer LDA considers an alternative objective. It does away with both the GMM and the shared covariance



(a) Noise in augmentation

(b) Variance orthogonal to S_F

(c) Dimension of projected space

Figure 4: We further extend the results presented in Fig 2 with orthonormalized InfoNCE and SimSiam mappings

assumption and assumes data to be coming from two different distributions, where each distribution belonged is defined by it's class. Fisher defined the separation between these two distributions to be the ratio of the variance between the classes to the variance within the classes i.e.

$$\mathcal{S}_{fisher} = \frac{|\boldsymbol{\theta}^T(\boldsymbol{\mu}_1 - \boldsymbol{\mu}_2)|^2}{|\boldsymbol{\theta}^T(w_1\boldsymbol{\Sigma}_1 + w_2\boldsymbol{\Sigma}_2)\boldsymbol{\theta}|}$$

The solution maximizing this is given by $(\boldsymbol{\Sigma}_1 + \boldsymbol{\Sigma}_2)^{-1}(\boldsymbol{\mu}_1 - \boldsymbol{\mu}_2)$ is termed the Fisher subspace. When the data is generated from a two-component shared covariance GMM, the solution coincides with $\boldsymbol{\Sigma}^{-1}(\boldsymbol{\mu}_1 - \boldsymbol{\mu}_2)$ learnt by LDA.